

Non-Hebbian plasticity transforms transient experiences into lasting memories

Reviewed Preprint

Revised by authors after peer review.

About eLife's process

Reviewed preprint version 2

April 29, 2024 (this version)

Reviewed preprint version 1

November 2, 2023

Posted to preprint server

August 15, 2023

Sent for peer review

August 14, 2023

Islam Faress, Valentina Khalil, Wen-Hsien Hou, Andrea Moreno, Niels Andersen, Rosalina Fonseca, Joaquin Piriz, Marco Capogna, Sadegh Nabavi 

Department of Molecular Biology and Genetics, Aarhus University, Aarhus, Denmark • Department of Biomedicine, Aarhus University, Aarhus, Denmark • DANDRITE, The Danish Research Institute of Translational Neuroscience, Aarhus University, Aarhus, Denmark • Center for Proteins in Memory – PROMEMO, Danish National Research Foundation,, Aarhus University, Aarhus, Denmark • Cellular and Systems Neurobiology, Universidade Nova de Lisboa, Portugal • Instituto de Fisiología Biología Molecular y Neurociencias (IFIBYNE), Universidad de Buenos Aires, CONICET, Buenos Aires, Argentina

 https://en.wikipedia.org/wiki/Open_access

 Copyright information

Abstract

The dominant models of learning and memory, such as Hebbian plasticity, propose that experiences are transformed into memories through input-specific synaptic plasticity at the time of learning. However, synaptic plasticity is neither strictly input specific nor restricted to the time of its induction. The impact of such forms of non-Hebbian plasticity on memory has been difficult to test, hence poorly understood. Here, we demonstrate that synaptic manipulations can deviate from the Hebbian model of learning, yet produce a lasting memory. First, we established a weak associative conditioning protocol, where optogenetic stimulation of sensory thalamic input to the amygdala was paired with a footshock, but no detectable memory was formed. However, when the same input was potentiated minutes before or after, or even 24 hours later, the associative experience was converted to a lasting memory. Importantly, potentiating an independent input to the amygdala minutes but not 24 hours after the pairing produced a lasting memory. Thus, our findings suggest that the process of transformation of a transient experience into a memory is neither restricted to the time of the experience nor to the synapses triggered by it; instead, it can be influenced by past and future events.

eLife assessment

This study presents **important** novel findings on how heterosynaptic plasticity can transform a weak associative memory into a stronger one, or produce a memory when stimuli were not paired. This work expands our views on the role of temporal- and input-specific plasticity in shaping learning and memory processes. The evidence, based on state-of-the-art in vivo manipulations, activity recordings, and behavioral analysis, is **convincing**. Findings will be of broad interest to neuroscience community, and especially those studying synaptic plasticity and associative memory.

Experience-dependent synaptic plasticity is widely regarded as the substrate of learning (Kandel et al., 2016; Mayford et al., 2012; Squire and Kandel, 2009), but see (Gallistel and King, 2009; Gershman, 2023). The dominant cellular model of learning, Hebbian plasticity, requires temporal and spatial specificity: the strength of a memory can be modified temporally only at the time of learning and spatially only at the encoding synapse and no other (Malenka and Bear, 2004; Maxwell Cowan et al., 2003). The most studied form of such plasticity is homo-synaptic long-term potentiation (homoLTP) of synaptic transmission or, as commonly known, LTP (Malenka and Bear, 2004; Maxwell Cowan et al., 2003). However, synaptic plasticity is neither temporally restricted to the time of the induction of the potentiation nor it is spatially confined to a single synapse (Harvey and Svoboda, 2007; Koch, 2004; Stuart et al., 2016; Yuste, 2010). Conceivably, therefore, the strength of a memory outside the time of learning can be modified by synaptic potentiation at the encoding synaptic input (homoLTP) or even in an independent input (heterosynaptic LTP, heteroLTP).

HeteroLTP has been identified in various synaptic pathways where a transient LTP can be stabilized by the induction of a more stable form of LTP on other synaptic inputs (Fonseca, 2013; Frey et al., 2001; Frey and Morris, 1997a; Shires et al., 2012). HeteroLTP is not limited to the synapses that are already potentiated. In fact, heteroLTP can be induced in non-potentiated synapses as long as they receive subthreshold stimuli (Harvey et al., 2008; Harvey and Svoboda, 2007; Hedrick et al., 2016; Murakoshi et al., 2011). Subsequent studies established a temporal window, ranging from minutes to tens of minutes, within which heteroLTP can be induced (Bear, 1997; Clopath et al., 2008; Govindarajan et al., 2006; Kastellakis et al., 2016; Kastellakis and Poirazi, 2019; O'Donnell and Sejnowski, 2014; Redondo and Morris, 2011). Thus, an LTP protocol can produce synaptic potentiation at the stimulated synapses (Hebbian homoLTP), but it also modulates plasticity at other synapses that converge onto the same neuron (non-Hebbian heteroLTP). Consequently, the phenomenon of heteroLTP may accompany a homoLTP but remain undetected.

This has motivated us to examine the impact of LTP stimuli delivered to one set of synapses on memories formed by inputs to the same or a convergent set of synapses. Specifically, we asked if the two forms of plasticity (Hebbian homoLTP and non-Hebbian heteroLTP) differ in their efficacy in converting a transient experience to a lasting memory; and if the time window between the experience and the induction of plasticity influences the stabilization of the memory. In this work, we performed a side-by-side comparison between the Hebbian and non-Hebbian forms of LTP to answer these questions. We observed that the non-Hebbian form of plasticity which deviates from Hebbian rules is effective in stabilizing an otherwise transient aversive experience.

Results

Rationale for the approaches taken in this study

In general, to establish a causal link between changes in synaptic weight to the memory strength, we must fulfill a set of criteria. First, one must know which synapses encode the memory (Stevens, 1998). For this, it is necessary to probe the synaptic inputs whose strength can be measured and modified. One must further show that modifying these inputs produces a quantifiable behavioral readout (Abdou et al., 2018; Jeong et al., 2021; Kim and Cho, 2017; Klavir et al., 2017; Nabavi et al., 2014; Roy et al., 2016; Zhou et al., 2017). Additionally, to test the effect of heteroLTP, one must induce plasticity on an independent synaptic input that modifies the strength of the memory. This independent activation requires a means to selectively and independently activate the two synaptic inputs—a nontrivial task in an *in vivo* preparation (Klapoetke et al., 2014).

To investigate the temporal and spatial properties of non-Hebbian plasticity in relation to memory and behavior, we chose the defensive circuit in the lateral amygdala (Fanselow and Poulos, 2005; Herry and Johansen, 2014; Janak and Tye, 2015; LeDoux, 2000; Maren and Quirk, 2004; Nabavi et al., 2014; Pape and Pare, 2010; Sah et al., 2008; Stevens, 1998; Tovote et al., 2015). First, most of its excitatory neurons receive inputs from two sources, thalamus and auditory/associative cortex (Choi et al., 2021; Humeau et al., 2005). Second, when these neurons receive a neutral conditioned stimulus (tone, CS) followed by an aversive unconditioned stimulus (shock, US), their synapses are potentiated to encode a memory of the aversive experience (conditioned response, CR) (Fanselow and Poulos, 2005; Herry and Johansen, 2014; Janak and Tye, 2015; LeDoux, 2000; Maren and Quirk, 2004; Pape and Pare, 2010; Sah et al., 2008; Tovote et al., 2015). To gain synapse-specific access to the CS input, we replaced a tone with optogenetic stimulation of the thalamic input (Jeong et al., 2021; Kim and Cho, 2017; Nabavi et al., 2014). This allowed precise control and monitoring of the strength of the synaptic inputs encoding the memory (Jeong et al., 2021; Kim and Cho, 2017; Nabavi et al., 2014).

Weak associative conditioning does not produce a lasting memory

The main objective of this work is to examine the efficacy of different forms of LTP in producing a lasting memory of an otherwise transient experience. Therefore, the memory under investigation must, by its nature, not be a lasting one. We have previously shown that an enduring CR can be produced by multiple pairs of optical co-activation of thalamic and auditory/associative cortical inputs with a footshock (Nabavi et al., 2014). We reasoned that reducing the number of pairings as well as the duration of the footshock should result in a less robust CR. As will become clear later, here we must be able to produce a CR by using only one input. Therefore, we asked whether pairing optical activation of thalamic inputs alone with footshock can produce a lasting CR, and whether we can reduce the CR by using fewer pairings of CS and US, and with shorter US duration.

We injected an AAV virus expressing a fast, blue-shifted variant of channelrhodopsin, oChIEF (Lin et al., 2013), in the lateral thalamus. To optically activate the thalamic inputs to the LA, we implanted a fiber optic above the dorsal tip of the LA (Fig. 1a, Extended Data Fig. 1). An optical CS alone did not produce a CR (Extended Data Fig. 1b), whereas temporal (but not non-temporal) multiple pairings of the optical CS with a footshock produced a freezing response (CR) measured 24hrs later (60 ± 7), indicating the formation of a long-term associative memory (Extended Data Fig. 1b). Importantly, reducing the number of pairings with shorter US duration resulted in a significant reduction in the CR 24hrs following the conditioning (7 ± 2) (Fig. 1a,b, Extended Data Fig. 1b).

HomoLTP stimulus produces a lasting memory in weak associative conditioning

We next examined the efficacy of the LTP protocol in producing a long-term memory at different time points from the weak conditioning protocol. Delivering an optical LTP stimulus immediately before or after such a conditioning protocol on the same inputs (homoLTP) produced a lasting CR (Fig. 1b). Remarkably, a homoLTP stimulus, even when delivered 24hrs after the conditioning, could produce a rapid CR comparable in magnitude to that obtained with immediate homoLTP (Fig. 1a,b). HomoLTP was as effective in mice that were tested prior to the induction protocol as those that were not (Fig. 1b, Extended Data Fig. 1d,e). It is notable that a homoLTP stimulus in naïve animals failed to produce a CR (Extended Data Fig. 1b); whereas it did produce a CR as long as the animals received the conditioning protocol (Fig. 1b). To confirm that optical homoLTP protocol was producing the expected effect on synaptic strength, we performed an *in vivo* recording from the LA in anesthetized mice expressing oChIEF in the thalamic inputs. Brief light pulses at the recording site produced *in vivo* field potentials which were potentiated by optical homoLTP stimulus (Fig. 1c,d).

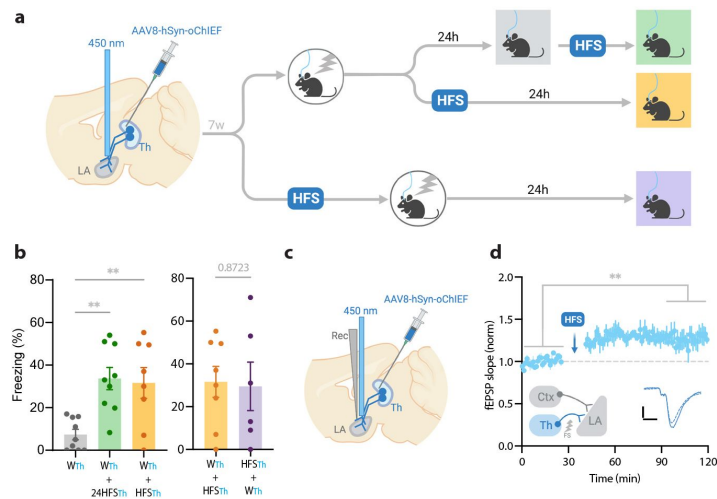


Figure 1.

Homosynaptic LTP stimulus minutes before, after, or 24 hrs after a weak associative conditioning produces lasting memory.

a) Diagram showing the experimental timeline. **b)** Left: High frequency stimulation (HFS) of the thalamic inputs (Th) to the lateral amygdala (LA) applied either 24 hours ($W_{Th}+24hHFS_{Th}$, corresponding to panel a, top branch), or immediately after a weak thalamic associative conditioning ($W_{Th}+HFS_{Th}$, corresponding to panel a, middle branch), significantly increased the CS-evoked freezing ($n=9$; One-way ANOVA, $F(2, 23) = 8.202$, $p\text{-value}=0.0020$) with Tukey test correction). Right: HFS of the thalamic input immediately before ($HFS_{Th}+W_{Th}$, corresponding to panel a, bottom branch) ($n=6$) or after a weak associative conditioning ($n=8$) ($W_{Th}+HFS_{Th}$, corresponding to panel a, middle branch) is equally effective in increasing the CS-evoked freezing. Colors of the bar graphs represent the experimental protocols for each group of mice (colored boxes in panel a). Subscripts with **blue font** indicate stimulation of the blue-shifted channelrhodopsin oChIEF using the selective procedure. **c)** Diagram showing the experimental setup of the *in vivo* electrophysiology recording (Rec) in anesthetized mice. Evoked field EPSP was produced by blue light stimulation (450nm) of the thalamic inputs expressing oChIEF. **d)** Plot of average *in vivo* field EPSP slope (normalized to baseline period) in the LA before and after HFS ($n=5$). Right inset: Superimposed traces of *in vivo* field responses to single optical stimulus before (dashed line) and after (solid line) HFS. Scale bar, 0.1 mV, 5ms. Results are reported as mean \pm S.E.M. **, $p<0.01$. Ctx: Cortical input; Th: Thalamic input; LA: lateral amygdala; HFS: High Frequency Stimulation; EPSP: excitatory postsynaptic potential; W_{Th} : Recall session after a weak thalamic associative conditioning.

Toward independent optical activation of thalamic and cortical inputs: Rendering a red-shifted channelrhodopsin insensitive to blue light

In addition to the thalamic inputs, most neurons within the LA receive direct projections from the cortical regions (auditory/associative) (Choi et al., 2021 [↗](#); Humeau et al., 2005 [↗](#)). We, therefore, asked whether synaptic potentiation on the cortical inputs (heteroLTP) following the weak conditioning of thalamic inputs is effective in producing a long-term CR, as predicted by computational models (O'Donnell and Sejnowski, 2014 [↗](#)).

Conceptually, the converging cortical and thalamic inputs to the LA can be activated independently using two opsins of distinct excitation spectra. The main obstacle is that all opsins, regardless of their preferred excitation spectrum, are activated by blue light (Klapoetke et al., 2014 [↗](#)). Recent attempts addressed this problem by pairing blue-light sensitive anion channels with red-shifted ChR2, where red light derives action potentials, while blue light, through shunting inhibition, nullifies the effect of the red-shifted ChR2 (Mermet-Joret et al., 2021 [↗](#); Vierock et al., 2021 [↗](#)). However, this approach, which is based on chloride influx, is not suitable for axonal terminal activation, where the chloride concentration is high (Mahn et al., 2018 [↗](#), 2016 [↗](#)).

A previous study demonstrated that prolonged illumination of axons expressing a red-shifted ChR2 reversibly renders the axons insensitive to further light excitation (Hooks et al., 2015 [↗](#)). We therefore tested whether thalamic axons expressing ChrimsonR can become transiently non-responsive to blue light by the co-illumination with a yellow light. It must be noted that yellow light minimally activates the blue shifted ChR2, oChIEF, (data not shown) the opsin that was later combined with ChrimsonR for independent optical activation of the thalamic and cortical axons. While activation of the thalamic axons expressing ChrimsonR by short pulses of blue light (10–15mW) was effective in evoking a field potential, the light failed to produce a discernible response when the illumination coincided with a 500ms yellow light of submilliwatt intensity. This was evident in whole cell recording from slices (**Fig. 2a–c** [↗](#)) as well as *in vivo* with single-pulse or high frequency stimulation (**Fig. 2d–h** [↗](#)). With the co-illumination, fiber volley and excitatory postsynaptic potential (the pre- and postsynaptic components, respectively) largely disappeared (**Fig. 2f** [↗](#)). The responses gradually recovered to their original values within hundreds of milliseconds (**Fig. 2f** [↗](#)). These data indicate that the observed insensitivity of ChrimsonR to blue light is more likely caused by the transient inactivation of the opsin rather than by the transmitter depletion or subthreshold depolarization of the axons. With an effective dual-color optical activation system at our disposal, we proceeded to investigate the effect of heteroLTP on the memory strength.

Immediate heteroLTP stimulus produces a lasting memory in weak associative conditioning

Mice were injected with AAV-ChrimsonR in the thalamic inputs and AAV-oChIEF in the cortical inputs to the LA (**Fig. 3a,b** [↗](#), **Extended Data Fig. 2a** [↗](#)). To optically activate either thalamic or cortical inputs, we implanted a fiber optic above the dorsal tip of the LA (**Extended Data Fig. 2a,b** [↗](#)). Within five minutes after weak conditioning on thalamic inputs, we delivered an optical LTP protocol on the cortical inputs (heterosynaptic LTP, heteroLTP), while blocking the activation of the thalamic inputs using the co-illumination. Mice were tested for their long-term memory retention 24hrs later (**Fig. 3a,b** [↗](#)). Similar to homoLTP, the induction of heteroLTP protocol immediately after the weak conditioning produced a long-term CR (**Fig. 3c** [↗](#)). In mice expressing opsin only in the thalamic inputs, the same manipulation failed to produce a CR (**Fig. 3c** [↗](#)). This demonstrates that the observed CR is caused by the heteroLTP.

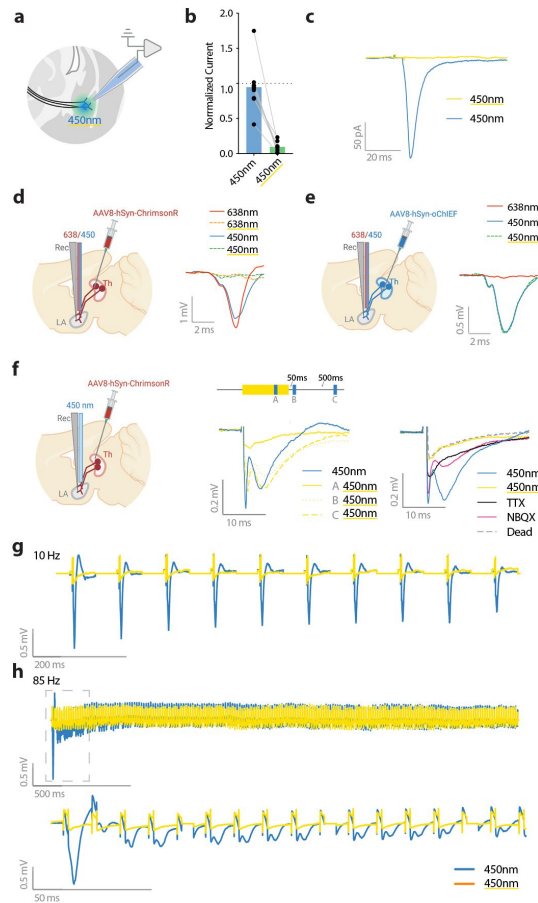


Figure 2.

Submilliwatt yellow light renders a red-shifted channelrhodopsin insensitive to blue light.

a) Diagram showing *ex vivo* electro-physiology recordings in slices where ChrimsonR-expressing thalamic inputs to the lateral amygdala (red lines) were optically activated. Synaptic responses were evoked by pulses of 450nm blue light (450nm), or pulses of blue light co-illuminated with a 561nm yellow light pulse (co-illumination). **b, c)** Bar graph (normalized to blue light (450nm) stimuli) (**b**), and example recording (scale bar, 50 pA, 20ms) (**c**), of optically driven synaptic responses to pulses of blue light (450nm) or pulses of blue light co-illuminated with yellow light (450nm with yellow underline) (2 animals, 3 slices, 7 cells). **d)** Left: Diagram showing the experimental set up of electrophysiology recordings in freely moving mice where ChrimsonR-expressing thalamic inputs (Th) to the lateral amygdala (LA) were optically activated. Right: Comparison of a representative waveform average of the response to pulses of red light (638nm), pulses of red light co-illuminated with a 500ms yellow light pulse (638nm with yellow underline), pulses of blue light (450nm), and pulses of blue light co-illuminated with a 500ms yellow light pulse (450nm with yellow underline) (n=3). **e)** Left: Diagram showing the experimental set up of electrophysiology recordings in freely moving mice where oChIEF-expressing thalamic inputs (Th) to the lateral amygdala (LA) were optically activated. Right: Comparison of a representative waveform average of the response to pulses of red light (638nm), pulses of blue light (450nm), and pulses of blue light co-illuminated with a 500ms yellow light pulse (450nm with yellow underline) (n=3). **f)** Left: Diagram showing the experimental setup of electrophysiology recordings in anesthetized mice where ChrimsonR-expressing thalamic inputs (Th) to the lateral amygdala (LA) were optically activated. Middle: Comparison of a representative waveform average of the response to pulses of blue light (450nm), pulses of blue light co-illuminated with a 500ms yellow light pulse (A), pulses of blue light following the yellow light pulse by 50 ms (B), or 500 ms (C) (n=4). Right: Comparison of the waveform average responses to pulses of blue light (450nm), pulses of blue light co-illuminated with a 500ms yellow light pulse (450nm with yellow underline), and pulses of blue light after sequentially applying NBQX and TTX, and later in a euthanized mouse (Dead), (n=4). Scale bar, 0.2 mV, 10ms. **g, h)** Representative traces for 10 Hz (**g**) and 85 Hz (**h**) stimulation of ChrimsonR-expressing thalamic inputs to the lateral amygdala, which were activated with blue light (450 nm, in blue). Yellow traces are the representative evoked responses of the inputs to 10 Hz (**g**) and 85 Hz (**h**) blue light stimulation (450 nm) co-illuminated with a 561nm yellow light pulse (n=3).

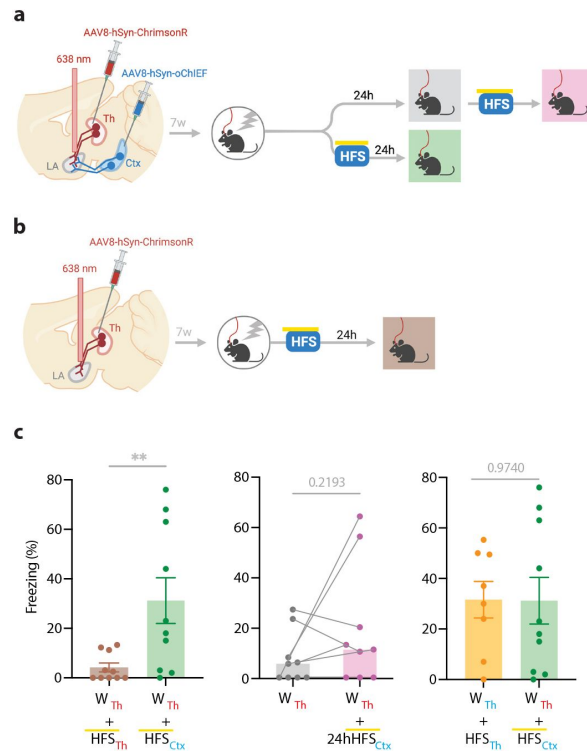


Figure 3.

Heterosynaptic LTP stimulus produces lasting memory if delivered within minutes after a weak associative conditioning.

a,b) Diagram showing the experimental timeline of the heterosynaptic LTP protocol manipulation following a weak thalamic associative conditioning. HFS with yellow upperline indicates that the delivery of high frequency stimulation with blue light overlapped with long pulses of yellow light. This co-illumination prevents the activation of ChrimsonR-expressing thalamic inputs (Th) by blue light, while the oChIEF-expressing cortical inputs remain unaffected. Note that yellow light specifically renders ChrimsonR, and not oChIEF, insensitive to blue light. **c)** Left: High frequency stimulation (HFS) of the thalamic input expressing ChrimsonR immediately following a weak associative conditioning on the same input ($W_{Th}+HFS_{Th}$, corresponding to panel b) ($n=9$) was ineffective in producing the CS-evoked freezing. HFS with yellow upperline indicates that HFS with blue light overlapped with long pulses of yellow light. This was to prevent the activation of ChrimsonR-expressing thalamic inputs by blue light, as described above and detailed in **figure 2**. The same HFS protocol in mice that additionally expressed oChIEF in the cortical inputs ($W_{Th}+HFS_{Ctx}$, corresponding to panel a, bottom branch) ($n=10$), significantly increased the CS-evoked freezing (heterosynaptic LTP) (Unpaired t-test, p -value=0.0100). Middle: HFS on the cortical input, induced 24 hours after a weak associative conditioning ($W_{Th}+24hHFS_{Ctx}$, corresponding to panel a, top branch) was ineffective in producing the CS-evoked freezing ($n=9$; Paired t-test, p -value=0.2193). Right: Comparison of the effect of homo-synaptic LTP protocol ($W_{Th}+HFS_{Th}$) (same dataset from **figure 1b**) and heterosynaptic LTP protocol ($W_{Th}+HFS_{Ctx}$) (same dataset from panel c, left) (Unpaired t-test, p -value=0.9740). Results are reported as mean \pm S.E.M. **, $p < 0.01$. Subscripts with **red font** and **blue font** indicate stimulation of the red-shifted channelrhodopsin ChrimsonR and the blue-shifted channelrhodopsin oChIEF, respectively.

As shown in the previous section, the delivery of an LTP protocol on the conditioned input (homoLTP) strengthens the memory even if delivered with a 24hrs delay. We then investigated whether heteroLTP protocol similarly maintains its efficacy when a long period has elapsed since conditioning. Mice expressing AAV-ChrimsonR and AAV-oChIEF in the thalamic and cortical inputs received a weak conditioning protocol, followed 24hrs later by an LTP protocol on the cortical inputs **a b c** (heteroLTP) (**Fig. 3c**). In this condition, heteroLTP protocol, in contrast to homoLTP protocol, failed to produce a significant CR (**Fig. 1b** and **3c**).

Homo- and heteroLTP stimuli produce a lasting memory in unpaired conditioning

It has been shown that the thalamic → LA pathway, in addition to its role in the auditory-cued fear learning, is required for the formation of contextual fear memory (Barsy et al., 2020). This can be explained by the fact that the lateral thalamus, the thalamic gateway to the LA, collects signals from different brain regions of diverse modalities (Barsy et al., 2020; Kang et al., 2022; Khalil et al., 2023; Ledoux et al., 1987; Linke et al., 1999). We, therefore, asked if, in addition to cued associative conditioning, an LTP protocol can produce CR in an unpaired form of conditioning on the thalamic → LA pathway. First, we tested whether the thalamic inputs convey a footshock signal to the LA, which is a prerequisite for this paradigm. For this purpose, we took advantage of fiber photometry in freely moving mice. AAV virus expressing the genetically encoded Ca²⁺ indicator GCaMP7s (Dana et al., 2019) was expressed in the thalamic inputs. GCaMP signal was collected through a fiber optic implanted above the tip of the LA (**Fig. 4a**, **Extended Data Fig. 3a,b**). The time-locked GCaMP activity of the thalamic projections to the onset of the footshock was evident, demonstrating that the thalamic inputs convey the footshock signal to the LA (**Fig. 4b**), confirming previous findings (Barsy et al., 2020). To further confirm this, we recorded the activity of the LA during footshock in mice with ablated lateral thalamus. This was done by the co-injection of AAV vectors expressing DIO-ta-Capsase3 and Cre recombinase in the lateral medial thalamus and GCaMP8m (Zhang et al., 2023) postsynaptically in the basolateral amygdala (**Fig. 4c**, **Extended Data Fig. 3c,d**). The control group underwent the same procedure, but the thalamus was spared (no Cre-recombinase was injected). In the thalamic-lesioned mice, the footshock-evoked response in the LA was significantly reduced (**Fig. 4d**). This further demonstrates that the aversive signal to the LA is conveyed largely through the thalamic inputs.

Next, we asked whether the induction of synaptic potentiation in this pathway following an unpaired conditioning, where footshock is not paired with the CS, would produce a long-term CR. It must be noted that previously we have shown that this protocol does not produce a detectable post-conditioning synaptic potentiation (Nabavi et al., 2014). Mice expressing AAV-oChIEF in the thalamic inputs received optical homoLTP stimulus on these inputs either immediately or 24hrs after the unpaired conditioning (**Fig. 4e**). Immediate homoLTP stimulus, indeed, proved to be effective in producing a lasting CR even for the unpaired conditioning (**Fig. 4f**); it is noteworthy that neither unpaired conditioning alone, nor optical homoLTP stimulus in naïve animals produced a CR (**Extended Data Fig. 4a**). HomoLTP protocol when delivered 24hrs later, produced an increase in freezing; however, the value was not statistically significant (**Extended Data Fig. 4b**). This observation is consistent with a previous report using only the unconditioned stimulus footshock (Li et al., 2020). This phenomenon is distinct from the paired form of conditioning which is receptive to homoLTP manipulation irrespective of the time of the delivery (**Fig. 1b**).

Next, we investigated the behavioral consequence of heteroLTP stimulus on the unpaired conditioning. Mice expressing AAV-ChrimsonR in the thalamic and AAV-oChIEF in the cortical inputs received optical LTP stimulus on the cortical inputs immediately after footshocks (**Fig. 4g**, **Extended Data Fig. 4c**). In this group, heteroLTP protocol produced a CR, which was comparable in magnitude to the paired conditioned animals (compare **Fig. 4h** with **Fig. 3c**).

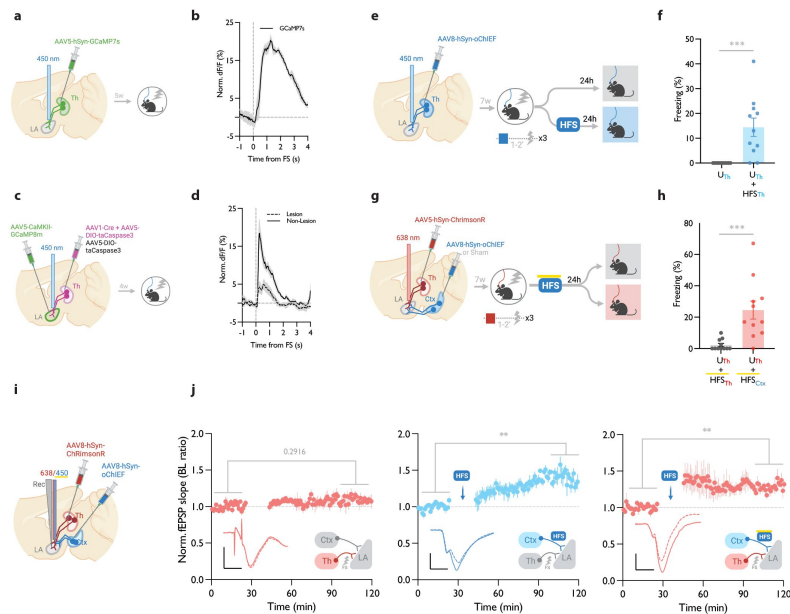


Figure 4.

Homosynaptic and heterosynaptic LTP protocols produce lasting memory when applied within minutes after an unpaired conditioning.

a) Diagram showing the experimental timelines for fiber photometry from the thalamic inputs (Th) expressing GCaMP7s. **b)** Averaged trace of the thalamic input activity in response to footshock (onset indicated by the dotted line), $n=5$. **c)** Diagram showing the experimental timelines for fiber photometry from the lateral amygdala (LA) neurons expressing GCaMP8m with intact or lesioned thalamic inputs. **d)** Averaged trace of the LA neurons activity in response to footshock (onset indicated by the dotted line) in mice with lesion (dash line) or no lesion (solid line) in the lateral thalamus (Th), $n=6$ per group. **e)** Diagram showing the experimental timelines of the homosynaptic LTP protocol manipulation following an unpaired thalamic conditioning. **f)** Unpaired conditioning on the thalamic inputs (U_{Th} , corresponding to panel e, top branch) produced no CS-evoked freezing, while if unpaired conditioning was immediately followed by high frequency stimulation (HFS) on the same inputs ($U_{Th}+HFS_{Th}$, corresponding to panel e, bottom branch) it significantly increased the CS-evoked freezing (homosynaptic LTP), ($n=11$ per group; Mann-Whitney test, p -value=0.0002). Subscripts with **blue font** indicate stimulation of the blue-shifted channelrhodopsin oChIEF using the selective procedure. **g)** Diagram showing the experimental timelines of the heterosynaptic LTP protocol manipulation following an unpaired thalamic conditioning. **h)** High frequency stimulation (HFS) of the thalamic input expressing red-shifted channelrhodopsin ChrimsonR immediately following an unpaired conditioning on the same input ($U_{Th}+HFS_{Th}$, corresponding to panel g, top branch) was ineffective in producing the CS-evoked freezing, while the same protocol in mice that, in addition, expressed oChIEF in the cortical inputs ($U_{Th}+HFS_{Ctx}$, corresponding to panel g, bottom branch), significantly increased the CS-evoked freezing (heterosynaptic LTP), ($n=11$ per group; Mann-Whitney test, p -value=0.0002). During HFS, blue light pulses overlapped with long pulses of yellow light. This co-illumination prevents the activation of ChrimsonR-expressing thalamic inputs (Th) by blue light, while the oChIEF-expressing cortical inputs remain unaffected. Note that yellow light specifically renders ChrimsonR, and not oChIEF, insensitive to blue light. Subscripts with **red font** and **blue font** indicate stimulation of the red-shifted channelrhodopsin ChrimsonR and the blue-shifted channelrhodopsin oChIEF, respectively. **i)** Diagram showing the experimental setup of the *in vivo* electrophysiology recordings (Rec) in anesthetized mice where the thalamic input expressing ChrimsonR and/or the cortical input expressing oChIEF were optically activated independently. **j)** Left: Plot of average *in vivo* field EPSP slope (normalized to baseline period) in the LA evoked by optical activation of the thalamic inputs, before and after footshock delivery ($n=5$; Paired t-test, p -value=0.2916). Middle: Plot of average *in vivo* field EPSP slope (normalized to baseline period) in the LA evoked by optical activation of the cortical inputs (Ctx), before and after high frequency stimulation (HFS) of these inputs ($n=6$; Paired t-test, p -value=0.0031). Right: Plot of average *in vivo* field EPSP slope (normalized to baseline period) in the LA evoked by optical activation of the thalamic inputs (Th), before and after HFS delivery on the cortical inputs (heterosynaptic LTP) ($n=5$; Paired t-test, p -value=0.0074). HFS with yellow upperline indicates that the delivery of high frequency stimulation with blue light overlapped with long pulses of yellow light. This co-illumination prevents the activation of ChrimsonR-expressing thalamic inputs (Th) by blue light, while the oChIEF-expressing cortical inputs remain unaffected. Superimposed traces of *in vivo* field response to single optical stimulus before (dash line) and after (solid line) the induced protocols. Results are reported as mean \pm S.E.M. **, $p < 0.01$; ***, $p < 0.001$.

Based on this observation, we asked whether heteroLTP stimulus can induce potentiation in the thalamic synaptic inputs which were activated merely by footshock. Indeed, we observed that following footshocks, optical LTP delivery on the cortical inputs induced lasting potentiation on the thalamic pathway despite the fact that footshock on its own did not produce any detectable form of postsynaptic potentiation (**Fig. 4i,j**). Without a footshock, high-frequency stimulation (HFS) of the cortical inputs did not induce synaptic potentiation on the thalamic pathway (**Extended Data Fig. 4d**). Therefore, although footshock on its own does not produce a detectable synaptic potentiation in thalamic inputs, it is required for heterosynaptic potentiation of this pathway.

HeteroLTP stimulus produces lasting potentiation of synaptic inputs encoding memory in weak associative conditioning

We and others have shown that optical LTP protocols produce expected behavioral changes (Nabavi et al., 2014; Roy et al., 2016; Zhou et al., 2017), such as strengthening a memory (**Fig. 1, 3, 4**). However, we considered these approaches insufficient to establish a direct behavioral correlate of synaptic changes. To determine if synaptic potentiation accompanies increased fear response following heteroLTP induction, we resorted to *in vivo* recording in freely moving mice. We expressed AAV-Chrim-sonR in the thalamic inputs, and AAV-oChIEF in the cortical inputs (**Extended Data Fig. 5a**). Six weeks after the injection, a customized optrode was implanted in the LA, which allows for the stimulation of the thalamic and cortical inputs as well as the measurement of the optically evoked field potential (**Fig. 5a, Extended Data Fig. 5b**).

The baseline for the evoked field potential and the input-output curve of both pathways were recorded prior to the conditioning (**Extended Data Fig. 5c**). Blue light pulses produced smaller evoked responses when coincided with submilliwatt long pulses of yellow light (data not shown). This further supports the efficacy of the dual optical activation approach that we adopted (**Fig. 2**), which permits independent activation of the converging thalamic and cortical inputs in behaving mice. To induce a weak conditioning protocol on the thalamic inputs, mice received red light stimulation co-terminated with a footshock (**Fig. 5a**). Within five minutes, we delivered an optical LTP protocol on the cortical inputs, while blocking the activation of the thalamic inputs using the co-illumination.

On the following day (recall day), we recorded evoked field responses prior to the memory retrieval. We observed a left shifted input-output curve as well as lasting potentiated field responses in both thalamic and cortical pathways (**Fig. 5b, Extended Data Fig. 5c**). Fifteen minutes later, mice were moved to a new context and tested for their memory recall by activating their thalamic inputs. Mice showed significantly increased freezing response during optical stimulation (**Fig. 5c**). A weak conditioning protocol that was not followed by an optical LTP protocol on the cortical inputs failed to produce synaptic potentiation of the thalamic inputs (tested 2hrs and 24hrs after the LTP protocol; **Extended Data Fig. 5d,e**).

HeteroLTP stimulus stabilizes a decaying form of synaptic potentiation in slices

Up to this point, we have shown that a memory and the underlying synaptic weight can be strengthened by the induction of LTP on an independent pathway. However, the notion of change in synaptic strength using an independent pathway was originally observed in slices (Fonseca, 2013; Frey and Morris, 1997b). We therefore tested if the two pathways which we used for our behavioral manipulations can undergo similar changes in synaptic weight in a slice preparation where we have a more precise control on the activation and monitoring of synaptic plasticity. Stimulation of the thalamic inputs with a weak induction protocol (**Fig. 5d**) resulted in a transient form of potentiation that regressed to the baseline within 90 minutes (**Fig. 5e**).

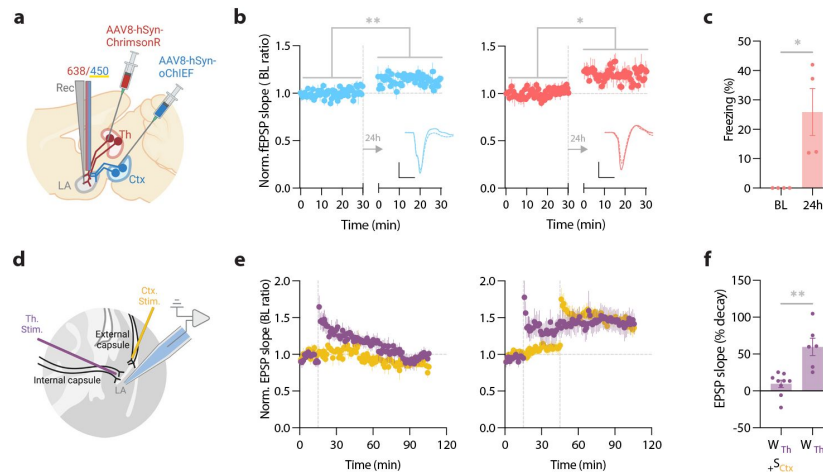


Figure 5.

Heterosynaptic LTP protocol when applied within minutes after a weak associative conditioning produces a long-lasting memory accompanied by the synaptic potentiation of the conditioned inputs.

a) Diagram showing the experimental setup of the *in vivo* electrophysiology recordings (Rec) in freely moving mice where the thalamic inputs expressing ChrimsonR and cortical inputs expressing oChIEF were optically activated independently. **b)** Left: Plot of average *in vivo* field EPSP slope (normalized to baseline period) in the LA evoked by optical activation of the cortical inputs, before and 24 hours after a weak thalamic conditioning followed immediately by HFS delivery on the same cortical inputs. Right: as left, except field EPSP was evoked by activation of the thalamic inputs. The potentiation of the field EPSP of the cortical (homosynaptic LTP) ($n=4$; Paired t-test, $p=0.0082$) as well as the thalamic inputs (heterosynaptic LTP), ($n=4$; Paired t-test, $p=0.0336$) is evident 24 hours after the delivery of HFS. Superimposed traces of *in vivo* field response to single optical stimulus before (dash line) and after (solid line) HFS. Scale bar, 0.5mV, 5ms. **c)** The behavioral responses of the mice tested for their homo- and hetero-synaptic plasticity in panel b. Note a significant CS-evoked freezing 24 hours after a weak thalamic conditioning followed immediately by HFS delivery on the cortical inputs (heterosynaptic LTP). These mice did not show a CS-evoked freezing prior to the protocol (BL) ($n=4$; Paired t-test, $p=0.0478$). **d)** Positioning of the stimulating electrodes (Th. Stim and Ctx. Stim.) and the recording electrode. **e)** (left) Weak stimulation of the thalamic inputs (purple circle) results in a transient LTP. No change was observed in the basal synaptic transmission of the cortical inputs (control pathway, yellow circle). Strong stimulation of the cortical inputs following the weak stimulation of the thalamic inputs stabilized synaptic potentiation of the thalamic inputs (right). Dash line indicates the onset of HFS induction. **f)** A paired-comparison of the decay of synaptic potentiation of the thalamic inputs with ($W_{Th}+S_{Ctx}$) or without (W_{Th}) the strong stimulation of the cortical inputs. ($n=4$; Welch's t test, $p=0.0062$). (10 animals, 15 slices; one cell per slice). Results are reported as mean \pm S.E.M. *, $p<0.05$; **, $p<0.01$.

However, when the weak conditioning protocol was followed by a strong conditioning protocol on the converging cortical inputs, it produced a stable form of potentiation that lasted for the entire duration of the recording (**Fig. 5e,f** [↗](#)).

Discussion

Numerous forms of synaptic plasticity, such as long-term potentiation (LTP) have been described but their relation to long-term memory is poorly understood. Here, we investigated the temporal and input specificity learning rules by which Hebbian and non-Hebbian forms of synaptic potentiation modify the strength of a memory. We found that the strength of a memory can be enhanced by potentiating the synaptic inputs encoding that memory (homoLTP) prior to or after an aversive conditioning. Importantly, we show that potentiation of an independent synaptic input (heteroLTP) minutes after the conditioning is as effective in strengthening the memory.

Our *in vivo* electrophysiology recordings from freely moving animals showed a strong correlation between synaptic potentiation and the successful recall of the aversive memory, as late as 24hrs after the induction of heteroLTP; all the mice with the successful recall had a successful potentiation of the synaptic input (**Fig. 5b,c** [↗](#)). This was accompanied by a lasting potentiation of the cortical input—the input that was used to induce heteroLTP in the thalamic inputs (**Fig. 5b** [↗](#)). Such a lasting behavioral and electrophysiological consequence of heteroLTP has not been reported before.

The efficacy of heteroLTP stimulus when delivered 24hrs after the conditioning drops considerably, whereas homoLTP retains its capacity to strengthen the memory. These data are consistent with the Synaptic Tagging and Capture (STC) model, which predicts that a heteroLTP protocol can stabilize a transient synaptic potentiation when induced minutes, but not hours prior to or after a weak LTP protocol (Redondo and Morris, 2011 [↗](#); Rogerson et al., 2014 [↗](#)).

Perhaps the most surprising finding in this work is that ho-moLTP as well as heteroLTP effectively uncover an aversive memory in an unpaired conditioning paradigm; this form of conditioning on its own does not produce a detectable memory (**Extended Data Fig. 4a** [↗](#)). It is important to note that previously we have shown that unpaired conditioning not only fails to produce a CR, but also does not induce synaptic potentiation, as predicted by Hebbian models of plasticity (Nabavi et al., 2014 [↗](#)). Similarly, in our *in vivo* recording, where anesthetized mice received multiple footshocks, no synaptic potentiation of thalamic inputs was detected (**Fig 4j** [↗](#)). The same protocol, however, when followed by heteroLTP stimulus, resulted in a synaptic potentiation that lasted for the entire duration of the recording (**Fig. 4j** [↗](#)). This is not predicted by the STC model in which heteroLTP works only on the already potentiated synaptic inputs. In this respect, this phenomenon is more in line with the Cross Talk model, which predicts heteroLTP can result in potentiation of synapses that have undergone subthreshold stimulation but no potentiation (Harvey et al., 2008 [↗](#); Harvey and Svoboda, 2007 [↗](#)). In the present context, the subthreshold activation could be the result of stimulation, and hence priming of the thalamic inputs by footshock. This is supported by the fact that in the absence of a footshock, LTP stimulus produces neither a CR nor a heterosynaptic potentiation (**Extended Data Fig. 4a,d** [↗](#)). As such, it appears that the mere potentiation of thalamic inputs is not sufficient to produce a memory, and some form of priming through associative or unpaired conditioning is essential.

Since we show that the thalamic inputs convey the footshock signal, the recovery of the CR following the LTP protocol on the same inputs (homoLTP) could be considered as a form of reinstatement, a well-known phenomenon where the mere presentation of a footshock after an extinguished CR reinstates the CR (Bouton, 2016; Bouton and Bolles, 1979 [↗](#)). We think this is

unlikely. First, we show that homoLTP is equally effective before the formation of the association. Additionally, we have shown previously that an LTP protocol is ineffective in restoring an extinguished CR (Nabavi et al., 2014 [↗](#)).

It must be noted that computational models simulating a circuit with comparable pre- and postsynaptic layouts to ours yield similar results; that is heteroLTP stabilizes a weak memory. However, according to these models, heteroLTP in brain circuits with different pre- and postsynaptic arrangements, may produce different physiological and behavioral outcomes (O'Donnell and Sejnowski, 2014 [↗](#)).

What cellular mechanisms could underlie the electrophysiological and behavioral phenomena we observed here? We consider some forms of postsynaptic intracellular diffusion from strongly stimulated cortical inputs to weakly stimulated neighboring thalamic inputs, as proposed by the Cross Talk and STC models. On the other hand, we consider the possibility of extra-cellular communication (Engert and Bonhoeffer, 1997 [↗](#)) such as glutamate spillover to be unlikely. Extracellular communication is mainly reported in the circuits at early developmental stages which lack a tight extracellular matrix sheath (Asztely et al., 1997 [↗](#)). Additionally, as we have shown here (**Extended Data Fig. 4d** [↗](#)) and reported by others (Doyère et al., 2003 [↗](#)), LTP induction on the cortical input produces no heterosynaptic effect on the naïve thalamic inputs. Taken together, our data point to an intracellular mechanism, which requires a prior priming but not necessarily a prior synaptic potentiation.

Consistent with this notion and complementary to our work, several studies have investigated the molecular and neuromodulatory mechanisms underlying endurance of memories. For example, it has been shown that exposure to a novel experience strengthens memory encoding in appetitive and aversive learning paradigms (Ballarini et al., 2009 [↗](#); Takeuchi et al., 2016 [↗](#)). Similarly, activation of dopaminergic inputs to the hippocampus after memory encoding enhances memory persistence, mimicking the effect of environmental novelty (Rossato et al., 2009 [↗](#); Takeuchi et al., 2016 [↗](#)). *De novo* protein synthesis dependence and/or neuromodulator-signaling were suggested to be essential for this phenomenon. At this stage, we have no ground to speculate about the molecular mechanisms underlying our observations. Further studies are needed to reveal the molecular machinery that enables non-Hebbian forms of plasticity that modify a memory and its synaptic strength across time and synapses.

Materials and Methods

Animals

Male mice of the strain C67BL/6JRj were purchased from Janvier Labs, France. Mice are purchased at the age of 6-8 weeks. All mice were housed in 12 hours light/dark cycle at 23 degrees Celsius and had *ad libitum* food and water access. Mice were housed 4 per cage. All procedures that involved the use of mice were approved by the Danish Animal Experiment Inspectorate.

Viruses

Recombinant adeno-associated viral vectors (AAV) were purchased from the viral vector facility VVF, at the University of Zurich, Switzerland. Serotype 8, AAV-2-hSyn1-oCHIEF_tdTomato(non-c.d.)-WPRESV40p(A) had physical titer of 6.6×10^{12} vg/mL. Serotype 5, AAV-1/2-hSyn1-chI-ChrimsonR_tdTomato-WPRESV40p(A) had physical titer of 5.3×10^{12} vg/mL. Serotype 5, AAV-2-mCaMKII α -jG-CaMP8m-WPRE-bGHp(A) had physical titer of 6.6×10^{12} vg/mL. Serotype 5, AAV-2-hSyn1-chI-jGCaMP7s-WPRESV40p(A) had physical titer of 7.7×10^{12} vg/mL. Serotype 5, ssAAV-2-hEF1 α -dlox-(pro)taCasp3_2A_TEVp(rev)-dlox-WPRE-hGHp(A) had physical titer of 4.7×10^{12}

vg/mL. Serotype 1, scAAV-1/2-hCMV-chI-Cre-SV40p(A)) had physical titer of 1.0×10^{13} vg/mL. Serotype 8, AAV-2-hSyn1-hM-4D(Gi)_mCherry-WPRE-hGHP(A) had physical titer of 4.8×10^{12} vg/mL.

Surgery

Mice were 7-9 weeks at the time of stereotaxic surgery. Mice were anesthetized with isoflurane and maintained at 1% throughout the surgery in the stereotaxic setup (Kopf 940) and a heating pad maintained body temperature at 37 degrees Celsius. Viruses were injected with a volume of 500-700 nL over 3-4 minutes. Auditory/associative cortex coordinates (all in mm and from Bregma) are (-2.85 AP, -4.4 ML and +1.6 DV (from the skull surface)). Lateral thalamus coordinates are (-3.15 AP, -1.85 ML and +3.5 DV (from the skull surface)). LA coordinates are (-1.65 AP, -3.45 ML and +3.45 DV (from the skull surface)). Optic fiber cannulas were cemented with dental cement, Super-bond (SUN MEDICAL, Japan). All the injections and optic fibers implantations were performed in the right hemisphere.

Optogenetics

ChR expressing AAVs were injected into the thalamic and the cortical regions projecting to the LA, and a 6-8 week expression time was given to allow for a high and stable expression in the axons. In freely moving mice, a 200 micrometer (Thorlabs 200 EMT, NA 0.39) optic fibers cannulae were implanted in the same surgery to target LA. The optic fiber cannulae were fabricated manually. The optic fiber was scored with an optic fiber scribe (Thorlabs s90 carbide scribe) and then pulled to break. Next, the optic fiber was inserted into the ferrule, and the output was measured with a power meter (Coherent Laser Check); 10 percent loss was the maximum allowed loss after coupling to the patch cord (Thorlabs 200 um NA 0.39). After-ward, the length was adjusted to 4mm (the exposed optic fiber) and glued with a UV curable glue. After gluing, the opposite end was scored and cut, and the output was measured again. The light output was confirmed to have a concentric-circle pattern.

In experiments with oChIEF, a 450 nm laser diode (Doric) was used with a light intensity of 10-15 mW. In the experiments with ChRimsonR, a 638 nm laser diode (Doric) was used with a light intensity of 10-15 mW, and a 561 nm laser diode (Vortran Laser Technology, USA) at the intensity of 1 mW for co-illumination when performing independent optical activation. All the freely moving experiments were done with a rotary joint (Doric Lenses, Canada). After each experiment, the verification of the brain stimulation location was performed after PFA fixation and slicing. For optimal optic fiber tract marking, the whole head of the mouse was left in 10% formalin for a week with agitation. Mice were excluded if the viral expression and/or the optic fiber locations were off target.

In vivo Electrophysiology

Mice were anesthetized with Urethane, Ethyl-Carbamate 2 mg/kg and placed in the stereotaxic setup, and a heating pad maintained the body temperature at 37 degrees Celsius. Multichannel system ME2100 was used for signal acquisition, and a Neuronexus opto-silicone probe with 32 channels was used to record the signal. Raw data were filtered (0.1–3000 Hz), amplified (100×), digitized, and stored (10 kHz sampling rate) for offline analysis with a tethered recording system (Multichannel Systems, Reutlingen, Germany). Analysis was performed using custom routines. The initial slope of field excitatory postsynaptic potentials was measured as described in [Nabavi et al., 2014](#).

The light-evoked signal was recorded from the LA in the right hemisphere. For LTP experiments, a baseline of the light-evoked fEPSP was measured for at least 20 minutes or until it was stable at 0.033 Hz, 1-2 ms pulses. At the of the baseline recording, 3 mild foot shocks were delivered to the mouse at the same intervals and intensity as the behavioral protocol. Only mice in **Extended Data**

Fig. 4d [↗](#) did not receive foot shocks. After the foot shock delivery, an HFS stimulation protocol was applied. The protocol consisted of 20 trains of 200 pulses of 2 ms, 450 nm light at 85 Hz with a 40-second inter-train interval. Immediately after the HFS, the light-evoked fEPSP was measured for at least 45 minutes to ensure the stability of the outcome of the LTP. This HFS protocol was used for all the experiments with HFS stimulation.

In the experiment that involved drug application, approximately 1 μ L of the drug (TTX: 10 ng or NBQX: 1 μ g) was applied onto the shank of the silicone probe and was inserted again. After each experiment, the brain recording location was verified through a stereoscope after PFA fixation and slicing.

For *in vivo* electrophysiological recordings from freely moving mice, a customized microdrive was designed to enable concurrent optical stimulation and recording of neuronal activity (modified from (Kvitsiani et al., 2013 [↗](#))). The microdrive was loaded with a single shuttle driving a bundle of 3 tetrodes (Sandvik) and one 200 μ m-diameter optical fiber (Doric lenses). Three weeks after virus injection, microdrive was implanted. For this, mice were anesthetized with 0.5 mg/kg FMM composed of the following mixture: 0.05 mg/ml of fentanyl ([Hameln, 007007] 0.05 mg/kg), 5 mg/mL of midazolam ([Hameln, 002124] 5 mg/kg), and 1 mg/mL of medetomidine (VM Pharma, 087896). To target the LA in the right hemisphere, a \sim 1mm diameter hole was drilled through the skull at the coordinates AP, -1.8 mm; ML, +3.4 mm. The microdrive was positioned with the help of a stereotaxic arm (Kopf Instruments) above the hole with protruding tetrodes. The optical fiber and tetrodes were gradually lowered to a depth of 500 μ m from the brain surface. A screw electrode was placed above the cerebellum to serve as the reference and ground electrode. The microdrive was secured to the skull with ultraviolet light curable dental cement (Vitrebond Plus) followed by a layer of Superbond (SUN MEDICAL). Tetrodes and the optical fiber were lowered by a further 2500 μ m before mice recovered from anesthesia. The post-operative analgesia Buprenorphine (0.1 mg/kg, S.C.) was administered 30 min before the end of surgery. Mice were allowed to recover for at least a week after the implantation.

Electrophysiological recordings were performed using a Neuralynx Cheetah 32 system. The electrical signal was sampled at 32 kHz and band-pass filtered between 0.1–8000 Hz.

Ex vivo slice electrophysiology (related to Fig. 2a-c [↗](#))

Experimental procedures were approved by the Animal Care and Use Committee of the University of Buenos Aires (CICUAL). Briefly, 4-week old C57 mice (n = 4) were injected with 250nl of AAV-1/2-hSyn1-chI-ChrimsonR_tdTomato-WPRE-SV40p at the MGN. After 3 weeks of expression, the animals were sacrificed and the brain removed and cut in 300 μ m coronal slices in a solution composed of (in mM): 92 N-Methyl-D-glucamine, 25 glucose, 30 NaHCO₃, 2.5 KCl, 1.25 NaH₂PO₄, 20 HEPES, 2 Thiourea, 5 Na-ascobate, 3 Na-pyruvate, 10 MgCl₂, and 0.5 CaCl₂ (equilibrated to pH 7.4 with 95% O₂–5% CO₂); chilled at 4°C. Slices containing the BLA were transferred to a 37 °C warmed chamber filled with the same solution and incubated for 10 minutes. After this period slices were transferred to a standard ACSF solution of composition (in mM): 126 NaCl, 26 NaHCO₃, 2.5 KCl, 1.25 NaH₂PO₄, 2 MgSO₄, 2 CaCl₂ and 10 Glucose (pH 7.4), at room temperature. Recordings started 1 hour later and were performed in this same ACSF solution. Patch-clamp recordings were done under a microscope (Nikon) connected to a Mightex Illumination system for 470 nm, and 532 nm light delivery. Whole-cell patch-clamp recordings were done using a K-gluconate based intracellular solution of the following composition (in mM): 130 K-gluconate, 5 KCl, 10 HEPES, 0.6 EGTA, 2.5 MgCl₂.6H₂O, 10 Phosphocreatine, 4 ATP-Mg, 0.4 GTP-Na₃. Glutamatergic AMPA mediated synaptic responses were recorded at -60 mV holding potential under blockage of GABA_A and NMDA receptors (Picrotoxin 100 μ M and APV 100 μ M). Light stimulation consisted in 2 ms pulses of 470 nm light at 10 mW, co-illumination consisted in 450 ms of 532 nm light at 1 mW that co-terminated with stimulation light.

Ex vivo slice electrophysiology (related to Fig. 5d-f [↗](#))

A total of 15 slices prepared from 10 Black6/J mice (3-5 week old) were used for electrophysiological recordings. All procedures were approved by the Portuguese Veterinary Office (Direcção Geral de Veterinária e Alimentação - DGAV). Coronal brain slices (300 μm) containing the lateral amygdala were prepared as described previously ([Fonseca, 2013 \[↗\]\(#\)](#)). Whole-cell current-clamp synaptic responses were recorded using glass electrodes (7-10M Ω ; Harvard apparatus, UK), filled with internal solution containing (in mM): K-gluconate 120, KCl 10, Hepes 15, Mg-ATP 3, Tris-GTP 0.3 Na-phosphocreatine 15, Creatine-Kinase 20U/ml (adjusted to 7.25 pH with KOH, 290mOsm). Putative pyramidal cells were selected by assessing their firing properties in response to steps of current. Only cells that had a resting potential of less than -60mV without holding current were taken further into the recordings. Neurons were kept at -70mV with a holding current below -0.25nA. In current clamp recordings, the series resistance was monitored throughout the experiment and ranged from 30M Ω -40M Ω . Electrophysiological data were collected using an RK-400 amplifier (Bio-Logic, France) filtered at 1 kHz and digitized at 10kHz using a Lab-PCI-6014 data acquisition board (National Instruments, Austin, TX) and stored on a PC. Offline data analysis was performed using a customized LabView-program (National Instruments, Austin, TX). To evoke synaptic EPSP, tungsten stimulating electrodes (Science Products, GmbH, Germany) were placed on afferent fibers from the internal capsule (thalamic input) and from the external capsule. Pathway independence was checked by applying two pulses with a 30ms interval to either thalamic or cortical inputs and confirming the absence of crossed pair-pulse facilitation. EPSPs were recorded with a test pulse frequency for each individual pathway of 0.033 Hz. After 15 min of baseline, transient LTP was induced with a weak tetanic stimulation (25 pulses at a frequency of 100 Hz, repeated three times with an interval of 3 sec) whereas long-lasting LTP was induced with a strong tetanic stimulation (25 pulses at a frequency of 100 Hz, repeated five times, with an interval of 3 sec).

As a measure of synaptic strength, the initial slope of the evoked EPSPs was calculated and expressed as percent changes from the baseline mean. Error bars denote SEM values. For the statistical analysis, LTP values were averaged over 5 min data bins immediately after LTP induction (T Initial) and at the end of the recording (T Final 95-100 minutes). LTP decay was calculated by $[(T \text{ Initial} - T \text{ Final})/T \text{ Final} * 100]$.

Fiber Photometry

GCaMP fluorescent signal was acquired by Doric fiber photometry system and through an optic fiber that is identical to the optogenetics ones described above. A pigtailed rotary joint (Doric) was used for all fiber photometry experiments in freely moving mice. Doric Lenses single site Fiber Photometry Systems with a standard 405/465 nm system fluorescent minicube iFMC4-G2_E(460-490)_F(500-540)_O(580-680)_S. The 405 nm was modulated at 208.616 Hz, and 465 nm was modulated at 572.205 Hz through the LED module driver. When the fiber photometry experiments were combined with optogenetics and/or electrophysiology recordings, the 638 nm laser diode was used to deliver the red light. A TTL generator device (Master 9) was used to time stamp the signals. The data was acquired through Doric Studio and analyzed in Doric studio and by a custom MatLab script. The code used for the analysis is freely available at the following link: [https://github.com/NabaviLab-Git/Photometry-Signal-Analysis \[↗\]\(#\)](https://github.com/NabaviLab-Git/Photometry-Signal-Analysis). Briefly, the signals were downsampled to 120 Hz using local averaging. A first order polynomial was fitted onto the data, using the least squares method. To calculate the relative change in fluorescence, the raw GCaMP signal was normalized using the fitted signal, according to the following equation: $\Delta F/F = (\text{GCaMP signal} - \text{fitted signal})/(\text{fitted signal})$. Behavioural events of interest were extracted and standardized using the mean and standard deviation of the baseline period.

Behavior

Eight weeks after the AAV injection, around 2 p.m., the mice were single-housed 20 minutes before the conditioning in identical cages to the home cages. Ugo Basile Aversive conditioning setup was used for all the experiments. The conditioning protocol was preceded by a pre-test, optical stimulation at 10 Hz for 30 seconds testing optical CS, identical to the one used in the 24-hours test. This step ensures that optical stimulation before conditioning and HFS does not cause any freezing or seizures. The strong conditioning protocol consisted of 5 pairings of a 2-seconds long optical CS at 10 hz, 20 pulses, co-terminated (last 15 pulses) with a 1.5-second foot shock 1 mA. The weak conditioning protocol was composed of 3 pairings of a 1.5-seconds long optical CS at 10 hz, 15 pulses, co-terminated (last 10 pulses) with a 1-second foot shock 1 mA. Twenty four hours later, the mice were tested in a modified context with bedding on the context floor, and chamber lights switched off. The mice were given a 2-minute baseline period or until they maintained a stable movement index and did not freeze at least 1 minute before the delivery of the testing optical CS. The testing optical CS was delivered twice, 2 minutes apart. Freezing was automatically measured through Anymaze (Stoelting, Ireland; version 5.3). Freezing percentages indicated the time the mouse spent freezing (in the 2 CSs) divided by 60 and multiplied by 100. The unpaired conditioning had the same number of pairings and parameters of the optical CS and the foot shock, as the weak conditioning protocol, with the difference that they were never paired, separated by 1 to 3 minutes.

Depending on the experiment, the HFS protocols (described above) were either delivered in the conditioning chamber with-in 5 minutes from the beginning or at the end of the conditioning session, or in testing chamber within 5 minutes from the end of the 24 hours recall. The control groups remained in the same context for the same amount of time as the mice that received the HFS protocol.

Drugs

All drugs were dissolved in sterile PBS from stock solutions. NBQX at 50 micromolar (Sigma) and TTX 0.5 micromolar (HelloBio) were added to the silicone probe's shank (5 microlitres). NBQX was added before the TTX.

Immunofluorescence

The mice were anesthetized with Iso-fluorane and euthanized by cervical dislocation. The heads were collected and stored for 7 days in 10% formalin at room temperature. Then, the brains were sliced into 100-120 μm thick slices in PBS on Leica Vibratome (VT1000 S).

To exclude any virus-mediated toxicity, the brains were stained for NeuN. Slices were permeabilized with PBS-Triton X 0.5% plus 10% of Normal Goat Serum (NGS; Thermo Fisher Scientific, 16210064) and blocked in 10% Bovine Goat Serum (BSA; Sigma, A9647) for 90 minutes at room temperature. Subsequently, the slices were incubated with anti-NeuN anti-body mouse (Merk Millipore, MAB377; 1:500) in PBS-Triton X 0.3%, 1% NGS, and 5% BSA. The incubation lasted for 72 hours at 4°C. At the end of the 72h incubation, the slices were washed three times in PBS at room temperature. Next, the slices were incubated in Cyanine 3 (Cy3) goat anti-mouse (Thermo Fisher Scientific, A10521, 1:500) in PBS-Triton X 0.3%, 1% NGS, and 5% BSA for 24 hours at 4°C. Finally, nuclear staining was performed using 1:1000 of DAPI (Sigma, D9542) for 30 minutes at room temperature. Brain slices were mounted on polysine glass slides (Thermo Scientific) with coverslips (Housein) using Fluoromount G (Southern Biotech) as mounting media.

Imaging

Imaging was performed by using a virtual slide scanner (Olympus VS120, Japan). Tile images were taken by the whole brain slides by using 10X (UPLSAPO 2 10x / 0,40) or 20X objective (UPLSAPO 20x / 0,75). The emission wavelength for Alexa 488 was 518 nm with 250 ms of exposure time. For Cy3, the emission wavelength was 565 nm with 250 ms of exposure time. The brain slices were visually inspected to confirm the virus expression in the thalamic and cortical regions projecting to the LA and to determine the optic fiber location in the LA.

Statistics

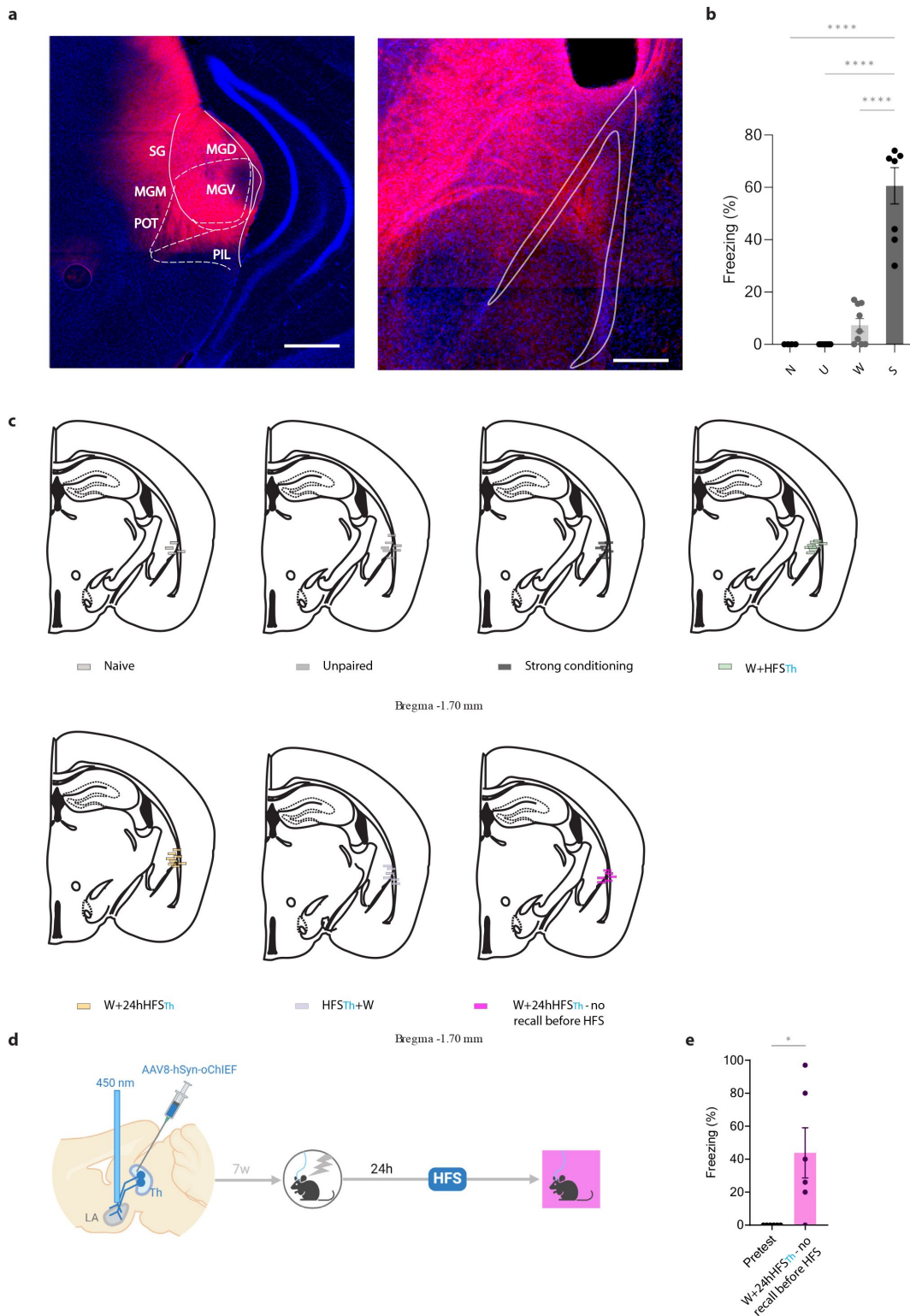
Statistical analyses were done via Prism 8.01 (Graph-Pad Software, San Diego, CA, USA). All the data are represented as mean \pm SEM. Before choosing the statistical test, a normality test (Shapiro-Wilk and D'Agostino-Pearson normality test) was done to all data sets. If the data presented a normal distribution, then a parametric test was used to calculate the statistical differences between groups. The statistical methods and the P values are mentioned in the figure legends.

Acknowledgements

We thank R. Malinow and the current and previous members of Nabavi laboratory for their suggestions during the progress of this project and their comments on the manuscript. We also thank R. Morris and P. Sterling for their comments on the manuscript. This study was supported by an ERC starting grant to S.N (22736), by Lundbeck NIH Brain Initiative grants to SN (R360-2021-650 and R273-2017-179) by the Danish Research Institute of Translational Neuroscience to S.N (19958), by PROMEMO (Center of Excellence for Proteins in Memory funded by the Danish National Research Foundation) to S.N (DNRF133). Figures were Created with *BioRender.com* [↗](#).

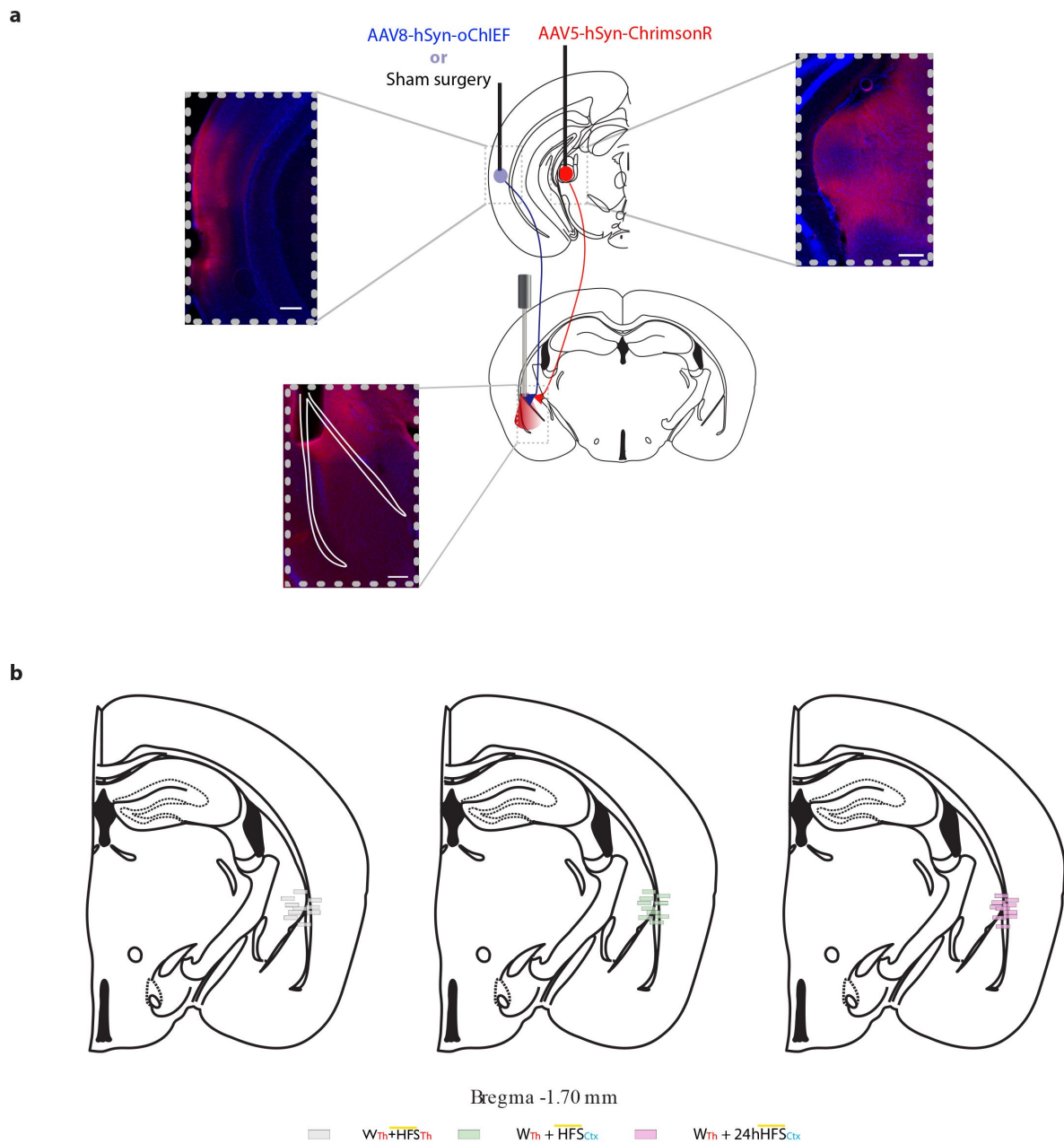
Contributions

SN conceived the project. SN and I.F designed the experiments. IF, VK, WHH, AM, NA, RF, and JP performed the experiments. AM and VK made the figures.



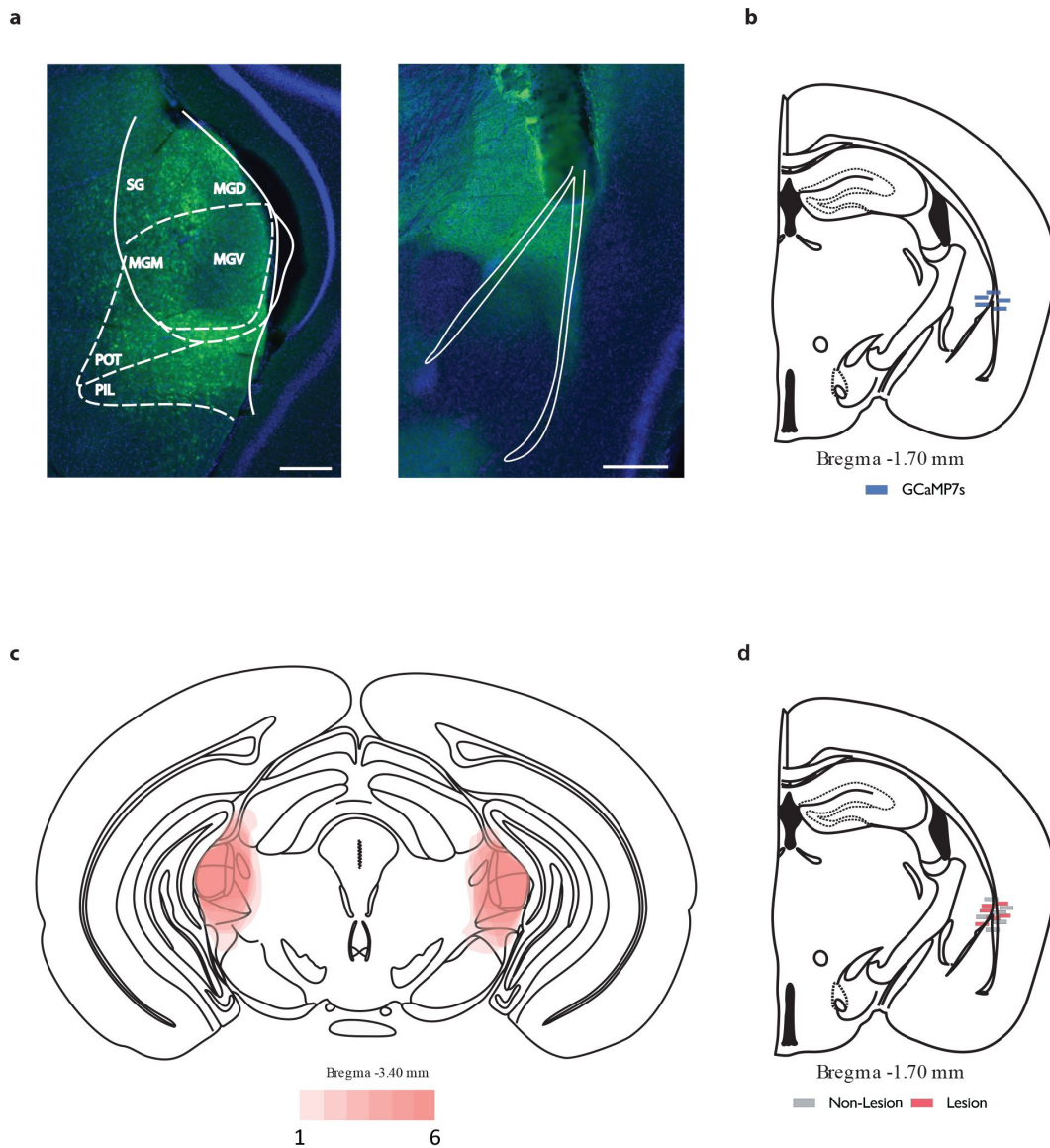
Extended data 1.

a) Representative image of a coronal section of mice expressing AAV-oChIEF-tdTomato in the lateral thalamus (Left). Scale bars, 1 mm. Axonal expression of AAV-oChIEF-tdTomato in the lateral amygdala (Right). Scale bars, 500 μ m. **b**) The CR is significantly higher after strong conditioning (S, n=8) compared to weak conditioning (W, n=9), and unpaired conditioning (U, n=7). Optical CS alone did not elicit any CR (N, n=4; Ordinary one-way ANOVA, $F(3, 28) = 60.79$, p -value < 0.0001 with Tukey test correction). **c**) Optic fiber placement of individual mice from **figure 1**. Results are reported as mean \pm S.E.M. ****, $p < 0.0001$.



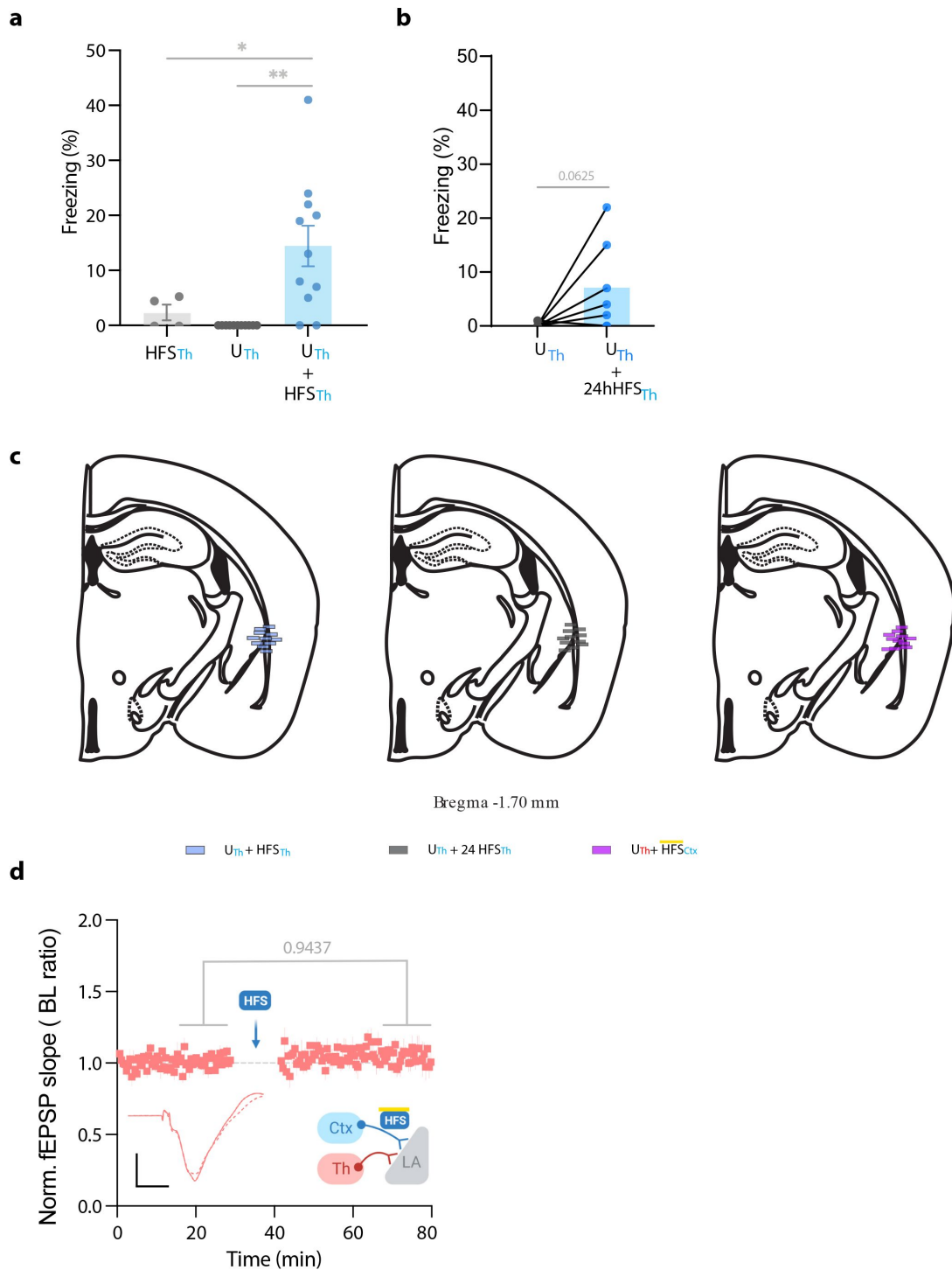
Extended data 2.

a) Representative image of a coronal section of mice expressing AAV-oChIEF-tdTomato in the LA-projecting cortical region and AAVChrimsonR-tdTomato in the LA-projecting thalamic region. Scale bars, 1 mm. Axonal expression of AAV-oChIEF-tdTomato and AAVChrimsonR-tdTomato in the lateral amygdala. Scale bars, 500 μ m. **b)** Optic fiber placement of individual mice from **figure 2**.



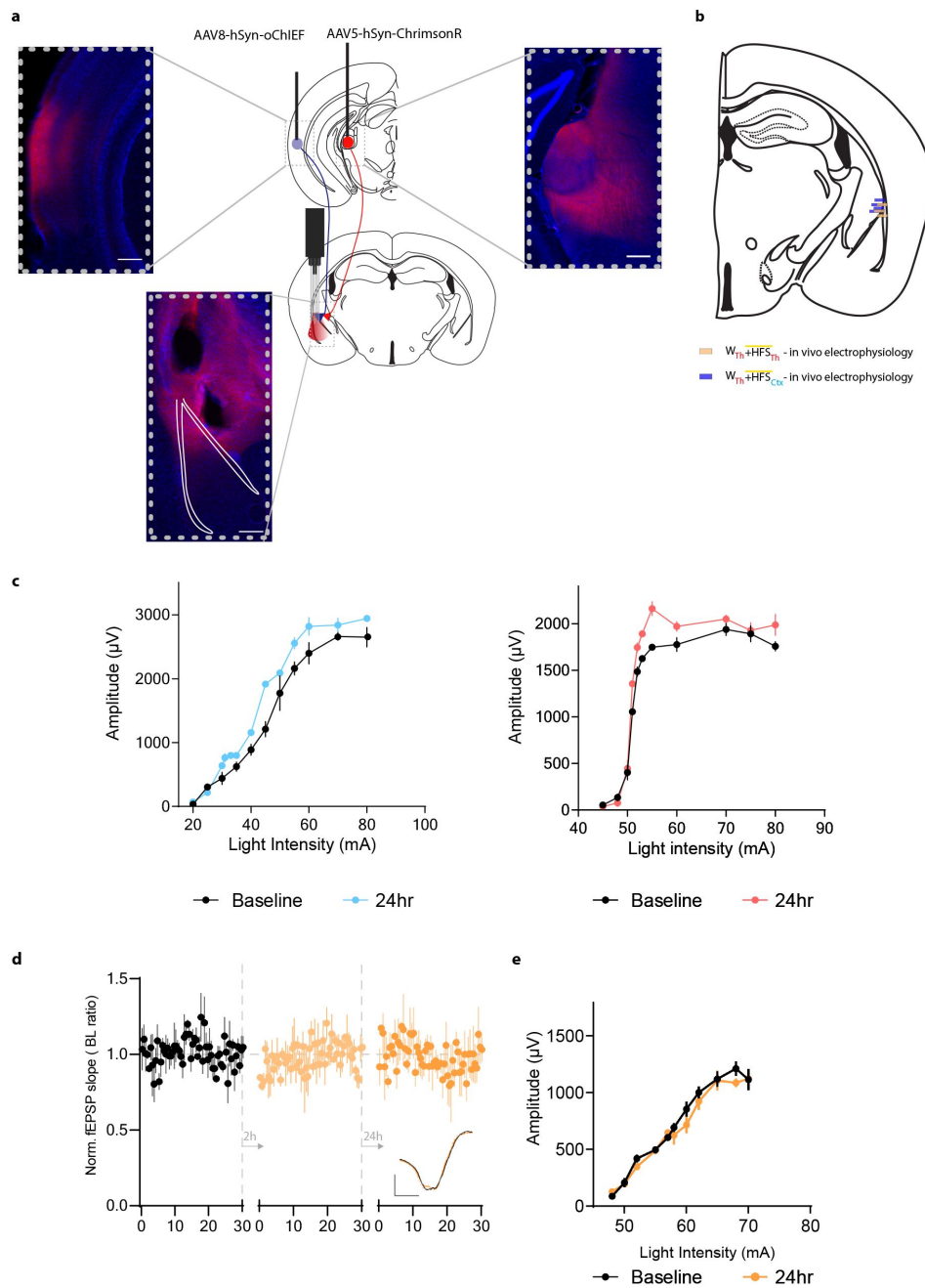
Extended data 3.

a) Representative image of a coronal section of mice expressing AAV-GCaMP7s in the lateral thalamus (Left). Scale bars, 1 mm. Axonal expression of AAV-GCaMP7s in the lateral amygdala. Scale bars, 500 μ m. **b)** Optic fiber placement of individual mice from [figure 3](#). **c)** Overlay of the maximum extent of the lesion in the thalamic-lesioned group (n=6). **d)** Optic fiber placement of individual mice from [figure 3](#) f,h.



Extended data 4.

a) Comparison of the freezing levels evoked by high frequency stimulation of the thalamic inputs in naive mice (HFS_{Th}, n=4) compared to mice subjected to unpaired conditioning (U; n=11) and to unpaired conditioning followed by HFS (U + HFS_{Th}, n=11; Ordinary one-way ANOVA, $F(2,23) = 10.09$, p-value=0.0007 with Tukey test correction). **b**) A paired comparison of the freezing levels evoked by thalamic axons activation when thalamic LTP is applied 24 hours after the unpaired conditioning (n=7, Wilcoxon test, p-value=0.0625). **c**) Optic fiber placement of individual mice from [figure 3](#). **d**) Plot for average *in vivo* field EPSP slope (normalized to baseline period) in the LA. The response was evoked by optical activation of the thalamic inputs (Th), before and after HFS delivery to the cortical inputs (heterosynaptic LTP) without delivering a foot shock (n=4; Paired t-test, p-value=0.9437). Results are reported as mean ± S.E.M.



Extended data 5.

a,b) Diagram and histology of the brain sections showing the AAVs injection sites, and the optrode implantation sites. **c)** Representative examples of the EPSP amplitude recorded in the LA by stimulation of cortical axons (left, repeated-measures Two-way RM ANOVA for group by light intensity, $F(1.752, 3.505) = 4.302$ p-value=0.1147 with Sidak test correction), and thalamic axons (right, repeated-measures Two-way RM ANOVA for group by light intensity, $F(1.936, 3.873) = 4.438$ p-value=0.0999 with Sidak test correction) before and after weak conditioning and cortical LTP. **d)** Plot for average *in vivo* field EPSP slope (normalized to baseline period) in the LA. Response was evoked by optical activation of the thalamic inputs before, 2hrs after, and 24hrs after a weak thalamic conditioning protocol. In the absence of HFS of the cortical inputs, there is no change in the field EPSP of the thalamic inputs ($n=3$; repeated-measures Two-way RM ANOVA for group by time interaction, $F(1.644, 3.288) = 0.8228$ p-value=0.4900 with Tukey correction). Superimposed traces of *in vivo* field response to single pulse optical stimulation before (black line), 2hrs after (dash orange line) and 24hrs after (solid orange line) HFS. **e)** Representative example of the EPSP amplitude recorded in the LA by stimulation of thalamic axons (repeated-measures Two-way RM ANOVA for group by light intensity, $F(10, 10) = 1.235$ p-value=0.3727). Results are reported as mean \pm S.E.M. #, $p<0.1$; **, $p<0.01$; ***, $p<0.001$.

References

- Abdou K, Shehata M, Choko K, Nishizono H, Matsuo M, Muramatsu S-I, Inokuchi K. (2018) **Synapse-specific representation of the identity of overlapping memory engrams** *Science* **360**:1227–1231
- Asztely F, Erdemli G, Kullmann DM (1997) **Extrasynaptic glutamate spillover in the hippocampus: dependence on temperature and the role of active glutamate uptake** *Neuron* **18**:281–293
- Ballarini F, Moncada D, Martinez MC, Alen N, Viola H. (2009) **Behavioral tagging is a general mechanism of long-term memory formation** *Proc Natl Acad Sci U S A* **106**:14599–14604
- Barsy B, Kocsis K, Magyar A, Babiczky Á, Szabó M, Veres JM, Hillier D, Ulbert I, Yizhar O, Mátyás F. (2020) **Associative and plastic thalamic signaling to the lateral amygdala controls fear behavior** *Nat Neurosci* **23**:625–637
- Bear MF (1997) **How do memories leave their mark?** *Nature*. Bouton ME. 2016 *Learning and Behavior*
- Bouton ME, Bolles RC (1979) **Role of conditioned contextual stimuli in reinstatement of extinguished fear** *J Exp Psychol Anim Behav Process* **5**:368–378
- Choi DI, Kim J, Lee H, Kim J-I, Sung Y, Choi JE, Venkat SJ, Park P, Jung H, Kaang B-K. (2021) **Synaptic correlates of associative fear memory in the lateral amygdala** *Neuron* **109**:2717–2726
- Clopath C, Ziegler L, Vasilaki E, Büsing L, Gerstner W. (2008) **Tag-trigger-consolidation: a model of early and late long-term-potential and depression** *PLoS Comput Biol* **4**
- Dana H *et al.* (2019) **High-performance calcium sensors for imaging activity in neuronal populations and microcompartments** *Nat Methods* **16**:649–657
- Doyère V, Schafe GE, Sigurdsson T, LeDoux JE (2003) **Long-term potentiation in freely moving rats reveals asymmetries in thalamic and cortical inputs to the lateral amygdala** *Eur J Neurosci* **17**:2703–2715
- Engert F, Bonhoeffer T. (1997) **Synapse specificity of long-term potentiation breaks down at short distances** *Nature* **388**:279–284
- Fanselow MS, Poulos AM (2005) **The neuroscience of mammalian associative learning** *Annu Rev Psychol* **56**:207–234
- Fonseca R. (2013) **Asymmetrical synaptic cooperation between cortical and thalamic inputs to the amygdala** *Neuropsychopharmacology* **38**:2675–2687
- Frey S, Bergado-Rosado J, Seidenbecher T, Pape HC, Frey JU (2001) **Reinforcement of early long-term potentiation (early-LTP) in dentate gyrus by stimulation of the basolateral amygdala: heterosynaptic induction mechanisms of late-LTP** *J Neurosci* **21**:3697–3703
- Frey U, Morris RG (1997) **Synaptic tagging and long-term potentiation** *Nature* **385**:533–536

- Frey U, Morris RG (1997) **Synaptic tagging and long-term potentiation** *Nature* **385**:533–536
- Gallistel CR, King AP (2009) **Memory and the Computational Brain: Why Cognitive Science will Transform Neuroscience**
- Gershman SJ (2023) **The molecular memory code and synaptic plasticity: A synthesis** *Biosystems* **224**
- Govindarajan A, Kelleher RJ, Tonegawa S. (2006) **A clustered plasticity model of long-term memory engrams** *Nat Rev Neurosci* **7**:575–583
- Harvey CD, Svoboda K. (2007) **Locally dynamic synaptic learning rules in pyramidal neuron dendrites** *Nature* **450**:1195–1200
- Harvey CD, Yasuda R, Zhong H, Svoboda K. (2008) **The spread of Ras activity triggered by activation of a single dendritic spine** *Science* **321**:136–140
- Hedrick NG, Harward SC, Hall CE, Murakoshi H, McNamara JO, Yasuda R. (2016) **Rho GTPase complementation underlies BDNF-dependent homo- and heterosynaptic plasticity** *Nature* **538**:104–108
- Herry C, Johansen JP (2014) **Encoding of fear learning and memory in distributed neuronal circuits** *Nat Neurosci* **17**:1644–1654
- Hooks BM, Lin JY, Guo C, Svoboda K. (2015) **Dual-channel circuit mapping reveals sensorimotor convergence in the primary motor cortex** *J Neurosci* **35**:4418–4426
- Humeau Y, Herry C, Kemp N, Shaban H, Fourcaudot E, Bissière S, Lüthi A. (2005) **Dendritic spine heterogeneity determines afferent-specific Hebbian plasticity in the amygdala** *Neuron* **45**:119–131
- Janak PH, Tye KM (2015) **From circuits to behaviour in the amygdala** *Nature* **517**:284–292
- Jeong Y, Cho H-Y, Kim M, Oh J-P, Kang MS, Yoo M, Lee H-S, Han J-H. (2021) **Synaptic plasticity-dependent competition rule influences memory formation** *Nat Commun* **12**:1–13
- Kandel ER, Dudai Y, Mayford MR (2016) **Learning and Memory: A Subject Collection from Cold Spring Harbor Perspectives in Biology**
- Kang SJ, Liu S, Ye M, Kim D-I, Pao GM, Copits BA, Roberts BZ, Lee K-F, Bruchas MR, Han S. (2022) **A central alarm system that gates multi-sensory innate threat cues to the amygdala** *Cell Rep* **40**
- Kastellakis G, Poirazi P. (2019) **Synaptic Clustering and Memory Formation** *Front Mol Neurosci* **12**
- Kastellakis G, Silva AJ, Poirazi P. (2016) **Linking Memories across Time via Neuronal and Dendritic Overlaps in Model Neurons with Active Dendrites** *Cell Rep* **17**:1491–1504
- Khalil V, Faress I, Mermet-Joret N, Kerwin P, Yonehara K, Nabavi S. (2023) **Subcortico-amygdala pathway processes innate and learned threats** *Elife* **12** <https://doi.org/10.7554/eLife.85459>

- Kim WB, Cho J-H. (2017) **Encoding of Discriminative Fear Memory by Input-Specific LTP in the Amygdala** *Neuron* **95**:1129–1146
- Klapoetke NC *et al.* (2014) **Independent optical excitation of distinct neural populations** *Nat Methods* **11**:338–346
- Klavir O, Prigge M, Sarel A, Paz R, Yizhar O. (2017) **Manipulating fear associations via optogenetic modulation of amygdala inputs to prefrontal cortex** *Nat Neurosci* **20**:836–844
- Koch C. (2004) **Biophysics of Computation** *Information Processing in Single Neurons*
- Kvitsiani D, Ranade S, Hangya B, Taniguchi H, Huang JZ, Kepecs A. (2013) **Distinct behavioural and network correlates of two interneuron types in prefrontal cortex** *Nature* **498**:363–366
- LeDoux JE (2000) **Emotion circuits in the brain** *Annu Rev Neurosci* **23**:155–184
- Ledoux JE, Ruggiero DA, Forest R, Stornetta R, Reis DJ (1987) **Topographic organization of convergent projections to the thalamus from the inferior colliculus and spinal cord in the rat** *J Comp Neurol* **264**:123–146
- Li F, Jia C-H, Huang J, Bi G-Q, Lau P-M. (2020) **High frequency optogenetic activation of inputs to the lateral amygdala forms distant association with foot-shock** *Mol Brain* **13**:1–4
- Lin JY, Knutsen PM, Muller A, Kleinfeld D, Tsien RY (2013) **ReaChR: a red-shifted variant of channelrhodopsin enables deep transcranial optogenetic excitation** *Nat Neurosci* **16**:1499–1508
- Linke R, De Lima AD, Schwegler H, Pape HC (1999) **Direct synaptic connections of axons from superior colliculus with identified thalamo-amygdaloid projection neurons in the rat: possible substrates of a subcortical visual pathway to the amygdala** *J Comp Neurol* **403**:158–170
- Mahn M, Gibor L, Patil P, Cohen-Kashi Malina K, Oring S, Printz Y, Levy R, Lampl I, Yizhar O. (2018) **High-efficiency optogenetic silencing with soma-targeted anion-conducting channelrhodopsins** *Nat Commun* **9**
- Mahn M, Prigge M, Ron S, Levy R, Yizhar O. (2016) **Biophysical constraints of optogenetic inhibition at presynaptic terminals** *Nat Neurosci* **19**:554–556
- Malenka RC, Bear MF (2004) **LTP and LTD: an embarrassment of riches** *Neuron* **44**:5–21
- Maren S, Quirk GJ (2004) **Neuronal signalling of fear memory** *Nat Rev Neurosci* **5**:844–852
- Maxwell Cowan W, Cowan WM, Südhof TC, Stevens CF (2003) **Synapses**
- Mayford M, Siegelbaum SA, Kandel ER (2012) **Synapses and memory storage** *Cold Spring Harb Perspect Biol* **4** <https://doi.org/10.1101/cshperspect.a005751>
- Mermet-Joret N, Moreno A, Zbela A, Ellendersen BE, Krauth N, von Philipsborn A, Piriz J, Lin JY, Nabavi S. (2021) **Dual-color optical activation and suppression of neurons with high temporal precision** *bioRxiv* <https://doi.org/10.1101/2021.05.05.442824>
- Murakoshi H, Wang H, Yasuda R. (2011) **Local, persistent activation of Rho GTPases during plasticity of single dendritic spines** *Nature* **472**:100–104

- Nabavi S, Fox R, Proulx CD, Lin JY, Tsien RY, Malinow R. (2014) **Engineering a memory with LTD and LTP** *Nature* **511**:348–352
- O'Donnell C, Sejnowski TJ (2014) **Selective memory generalization by spatial patterning of protein synthesis** *Neuron* **82**:398–412
- Pape H-C, Pare D. (2010) **Plastic synaptic networks of the amygdala for the acquisition, expression, and extinction of conditioned fear** *Physiol Rev* **90**:419–463
- Redondo RL, Morris RGM (2011) **Making memories last: the synaptic tagging and capture hypothesis** *Nat Rev Neurosci* **12**:17–30
- Rogerson T, Cai DJ, Frank A, Sano Y, Shobe J, Lopez-Aranda MF, Silva AJ (2014) **Synaptic tagging during memory allocation** *Nat Rev Neurosci* **15**:157–169
- Rossato JI, Bevilaqua LRM, Izquierdo I, Medina JH, Cammarota M. (2009) **Dopamine controls persistence of long-term memory storage** *Science* **325**:1017–1020
- Roy DS, Arons A, Mitchell TI, Pignatelli M, Ryan TJ, Tonegawa S. (2016) **Memory retrieval by activating engram cells in mouse models of early Alzheimer's disease** *Nature* **531**:508–512
- Sah P, Westbrook RF, Lüthi A. (2008) **Fear conditioning and long-term potentiation in the amygdala: what really is the connection?** *Ann N Y Acad Sci* **1129**:88–95
- Shires KL, Da Silva BM, Hawthorne JP, Morris RGM, Martin SJ (2012) **Synaptic tagging and capture in the living rat** *Nat Commun* **3**
- Squire LR, Kandel ER (2009) **Memory: From Mind to Molecules**
- Stevens CF (1998) **A million dollar question: does LTP = memory?** *Neuron* **20**:1–2
- Stuart G, Spruston N, Häusser M. (2016) **Dendrites**
- Takeuchi T *et al.* (2016) **Locus coeruleus and dopaminergic consolidation of everyday memory** *Nature* **537**:357–362
- Tovote P, Fadok JP, Lüthi A. (2015) **Neuronal circuits for fear and anxiety** *Nat Rev Neurosci* **16**:317–331
- Vierock J *et al.* (2021) **BiPOLES is an optogenetic tool developed for bidirectional dual-color control of neurons** *Nat Commun* **12**
- Yuste R. (2010) **Dendritic Spines**
- Zhang Y *et al.* (2023) **Fast and sensitive GCaMP calcium indicators for imaging neural populations** *Nature* <https://doi.org/10.1038/s41586-023-05828-9>
- Zhou T *et al.* (2017) **History of winning remodels thalamo-PFC circuit to reinforce social dominance** *Science* **357**:162–168

Article and author information

Islam Faress

Department of Molecular Biology and Genetics, Aarhus University, Aarhus, Denmark, Department of Biomedicine, Aarhus University, Aarhus, Denmark, DANDRITE, The Danish Research Institute of Translational Neuroscience, Aarhus University, Aarhus, Denmark, Center for Proteins in Memory – PROMEMO, Danish National Research Foundation,, Aarhus University, Aarhus, Denmark

Valentina Khalil

Department of Molecular Biology and Genetics, Aarhus University, Aarhus, Denmark, DANDRITE, The Danish Research Institute of Translational Neuroscience, Aarhus University, Aarhus, Denmark, Center for Proteins in Memory – PROMEMO, Danish National Research Foundation,, Aarhus University, Aarhus, Denmark

Wen-Hsien Hou

Department of Biomedicine, Aarhus University, Aarhus, Denmark

Andrea Moreno

Department of Molecular Biology and Genetics, Aarhus University, Aarhus, Denmark, DANDRITE, The Danish Research Institute of Translational Neuroscience, Aarhus University, Aarhus, Denmark, Center for Proteins in Memory – PROMEMO, Danish National Research Foundation,, Aarhus University, Aarhus, Denmark

Niels Andersen

Department of Molecular Biology and Genetics, Aarhus University, Aarhus, Denmark, DANDRITE, The Danish Research Institute of Translational Neuroscience, Aarhus University, Aarhus, Denmark, Center for Proteins in Memory – PROMEMO, Danish National Research Foundation,, Aarhus University, Aarhus, Denmark

Rosalina Fonseca

Cellular and Systems Neurobiology, Universidade Nova de Lisboa, Portugal

Joaquin Piriz

Instituto de Fisiología Biología Molecular y Neurociencias (IFIBYNE), Universidad de Buenos Aires, CONICET, Buenos Aires, Argentina

Marco Capogna

Department of Biomedicine, Aarhus University, Aarhus, Denmark, Center for Proteins in Memory – PROMEMO, Danish National Research Foundation,, Aarhus University, Aarhus, Denmark

Sadegh Nabavi

Department of Molecular Biology and Genetics, Aarhus University, Aarhus, Denmark, DANDRITE, The Danish Research Institute of Translational Neuroscience, Aarhus University, Aarhus, Denmark, Center for Proteins in Memory – PROMEMO, Danish National Research Foundation,, Aarhus University, Aarhus, Denmark

For correspondence: snabavi@dandrite.au.dk

Copyright

© 2023, Faress et al.

This article is distributed under the terms of the [Creative Commons Attribution License](#), which permits unrestricted use and redistribution provided that the original author and source are credited.

Editors

Reviewing Editor

Mihaela Iordanova

Concordia University, Montreal, Canada

Senior Editor

Kate Wassum

University of California, Los Angeles, Los Angeles, United States of America

Reviewer #1 (Public Review):

Summary:

The authors goal here was to explore how a non hebbian form of plasticity, heterosynaptic LTP, could shape neuronal responses and learning. They used several conceptually and technically innovative approaches to answer this. First, they identified a behavioral paradigm that was a subthreshold training paradigm (stimulation of thalamic inputs with a footshock), which could be 'converted' to a memory via homosynaptic LTP (HFS of thalamic inputs). They then find that stimulation of 'cortical' inputs could also convert the subthreshold stimulation to a lasting memory, and that this was associated with a change in neuronal response, akin to LTP. Finally, they provide some slice work which demonstrated that stimulation of cortical inputs could stabilize LTP at thalamic inputs.

Strengths:

- (1) The approach was innovative and asked an important question in the field.
- (2) The studies are, for the most part, quite rigorous, using a novel dual opsin approach to probe multiple inputs in vivo.
- (3) The authors explore neural responses both in vivo and ex vivo, as well as leveraging a 'simple' behavior output of freezing.

<https://doi.org/10.7554/eLife.91421.2.sa1>

Reviewer #2 (Public Review):

Summary

Faress et al. address how synaptic plasticity (i.e. potentiation induced by high frequency stimulation, HFS) induced at different time points and pathways relative to those active during initial learning can transform memories. They adopt an experimental design developed by Nabavi et al, 2014 to optogenetically induce a weak fear memory by pairing an optical conditioned stimulus (CS) at thalamo-LA synapses with a footshock unconditioned stimulus (US) in male mice. Homosynaptic HFS delivered in the same pathway before or after

conditioning transforms the weak memory into a stronger one. Leveraging a new dual wavelength optogenetic approach *in vivo*, they also show that heterosynaptic (cortico-LA) HFS directly following the opto-conditioning can transform the thalamo-LA induced fear memory, or create a memory when directly delivered after unpaired conditioning. Lastly, they demonstrate that heterosynaptic potentiation of the thalamo-LA pathway accompanies the strengthening of fear memory in freely moving mice. The authors conclude that a transient experience (i.e. weak memory) can be transformed into a stable one by non-Hebbian forms of plasticity.

Strengths

This study uses well-defined and elegant optogenetic manipulations of distinct neural pathways in awake behaving mice combined with *in vivo* recordings, which allows to directly manipulate and monitor synaptic strength and memory. It addresses an interesting, timely, and important question.

Weaknesses

A key experiment with *in vivo* monitoring of LFPs and behavior (Fig. 5a-c) seems a bit underpowered and input-output curves (extended data 5c) not entirely convincing. *Ex vivo* slice experiments (Fig. 5d-f) are not well aligned with *in vivo* experimental conditions. While they provide proof of principle, this is not entirely novel (see Fonseca et al, 2013).

Significance and impact

The conclusions are well supported by the data. The significance of the study lies in showing *in vivo*, that plasticity induced at different times or synaptic pathways than those engaged during learning can modify a memory and the synaptic strength in the neural pathway related to that memory. While heterosynaptic and timing-dependent effects in synaptic plasticity have been described largely *ex vivo* on shorter time scales, the discovery of lasting behavioral effects on memory is novel. The study was enabled by a combination of clever approaches: creation of a "synthetic" pathway-specific association and a novel dual opsin approach *in vivo* to probe the role of plasticity in a converging second pathway at the same time.

This work broadens our understanding of how Hebbian and non-Hebbian forms of plasticity shape neural activity and associative memory and is of broad interest to the neuroscience community.

<https://doi.org/10.7554/eLife.91421.2.sa0>

Author response:

The following is the authors' response to the original reviews.

Reviewer #1 (Public Review):

(1) There appears to be a flaw in the exploration of cortical inputs. the authors never show that HFS of cortical inputs has no effect in the absence of thalamic stimulation. It appears that there is a citation showing this, but I think it would be important to show this in this study as well.

We understand that the reviewer would like us to induce an HFS protocol on cortical input and then test if there is any change in synaptic strength in thalamic input. We have done this experiment which shows that without a footshock, high-frequency stimulation (HFS) of the

cortical inputs did not induce synaptic potentiation on the thalamic pathway (Extended Data Fig. 4d).

(2) It is somewhat confusing that the authors refer to the cortical input as driving heterosynaptic LTP, but this is not shown until Figure 4j, that after non-associative conditioning (unpaired shock and tone) HFS of the cortex can drive freezing and heterosynaptic LTP of thalamic inputs.

We agree with the reviewer that it is in figure 4j and figure 5,b,c which we show electrophysiological evidence for cortical input driving heterosynaptic LTP. It is only to be consistent with our terminology that initially we used behavioral evidence as the proxy for heteroLTP (figure 3c).

..., the authors are 'surprised' by this outcome, which appears to be what they predict.

We removed the phrase “To our surprise”.

(3) 'Cortex' as a stimulation site is vague. The authors have coordinates they used, it is unclear why they are not using standard anatomical nomenclature.

We replaced “cortex” with “auditory/associative cortex”.

(4) The authors' repeated use of homoLTP and heteroLTP to define the input that is being stimulated makes it challenging to understand the experimental detail. While I appreciate this is part of the goal, more descriptive words such as 'thalamic' and 'cortical' would make this much easier to understand.

We agree with the reviewer that a phrase such as “an LTP protocol on thalamic and cortical inputs” would be more descriptive. We chose the words “homoLTP” and “heteroLTP” only to clarify (for the readers) the physiological relevance of these protocols. We thought by using “thalamic” and “cortical” readers may miss this point. However, when for the first time we introduce the words “homoLTP” and “heteroLTP”, we describe which stimulated pathway each refers to.

Reviewer #2 (Public Review):

(1) ...The experimental schemes in Figs. 1 and 3 (and Fig. 4e and extended data 4a,b) show that one group of animals was subjected to retrieval in the test context at 24 h, then received HFS, which was then followed by a second retrieval session. With this design, it remains unclear what the HFS impacts when it is delivered between these two 24 h memory retrieval sessions.

We understand that the reviewer has raised the concern that the increase in freezing we observed after the HFS protocol (ex. Fig. 1b, the bar labeled as Wth+24hHFSth) could be caused or modulated by the recall prior to the HFS (Fig. 1a, top branch). To address this concern, in a new group of mice, 24 hours after weak conditioning, we induced the HFS protocol, followed by testing (that is, no testing prior to the HFS protocol). We observed that homoLTP was as effective in mice that were tested prior to the induction protocol as those that were not (Fig. 1b, Extended Data Fig. 1d,e).

It would be nice to see these data parsed out in a clean experimental design for all experiments (in Figs 1, 3, and 4), that means 4 groups with different treatments that are all tested only once at 24 h, and the appropriate statistical tests (ANOVA). This would also

avoid repeating data in different panels for different pairwise comparisons (Fig 1, Fig 3, Fig 4, and extended Fig 4).

While we understand the benefit of the reviewer's suggestion, the current presentation of the data was done to match the flow of the text and the delivery of the information throughout the manuscript. We think it is unlikely that the retrieval test prior to the HFS impacts its effectiveness, as confirmed by homosynaptic HFS data (Extended Data Fig. 1d,e). It is beyond the scope of current manuscript to investigate the mechanisms and manipulations related to reconsolidation and retrieval effects.

(2) ... It would be critical to know if LFPs change over 24 h in animals in which memory is not altered by HFS, and to see correlations between memory performance and LFP changes, as two animals displayed low freezing levels. ... They would suggest that thalamo-LA potentiation occurs directly after learning+HFS (which could be tested) and is maintained over 24 h.

We have performed the experiment where we recorded the evoked LFP 2hrs and 24hrs following the weak conditioning protocol. We observed that a weak conditioning protocol that was not followed by an optical LTP protocol on the cortical inputs failed to produce synaptic potentiation of the thalamic inputs (tested 2hrs and 24hrs after the LTP protocol; Extended Data Fig. 5d,e).

(3) The statistical analyses need to be clarified. All statements should be supported with statistical testing (e.g. extended data 5c, pg 7 stats are missing). The specific tests should be clearly stated throughout. For ANOVAs, the post-hoc tests and their outcomes should be stated. In some cases, 2-way ANOVAs were performed, but it seems there is only one independent variable, calling for one-way ANOVA.

All the statistical analyses have been revised and the post-hoc tests performed after the ANOVAs are mentioned in the relevant figure legends.

Reviewer #2 (Recommendations For The Authors):

The wording "transient" and "persistent" used here in the context of memory seems a bit misleading, as only one timepoint was assessed for memory recall (24 h), at which the memory strength (freezing levels) seem to change.

As the reviewer mentioned, we have tested memory recall only at one time point. For this reason, throughout the text we used "transient" exclusively to refer to the experience (receiving footshock) and not to the memory. We replaced "persistence" with "stabilization" where it refers to a memory ("the induction of plasticity influences the stabilization of the memory").

For the procedures in which the CS and US were not paired, the term "unpairing" is used (which is probably the more adequate one), but the term "non-associative conditioning" appears in the text, which seems a bit misleading, as this term may have another connotation. There is also literature that an unpairing of CS and US could lead to the formation of a safety memory to the CS, that may be disrupted by HFS stimulation.

We replaced "non-associative" with "unpaired".

Validation of viral injection sites for all experiments: Only representative examples are shown, it would be nice to see all viral expression sites.

For this manuscript, we have used 155 mice. For this reason, including the injection sites for all the animals in the manuscript is not feasible. Except for the mice that have been excluded, (please see exclusion criteria added in the methods), the expression pattern we observed was consistent across animals and therefore the images shown are true representatives.

Extended Data 1b: Please explain what N, U, W, and S behavioral groups mean. To what groups mentioned in the text (pg 2,3) do these correspond?

The requested clarifications are implemented in the figure legend.

Please elaborate on the following aspects of your methods and approaches:

- *Please explain if the protocol for HFS to manipulate behavior was the same as the one used for the LTP experiments (Fig 1d, Fig 4j) and was identical for homo/hetero inputs from thal and ctx?*

We used the same HFS protocol for all the HFS inductions. We included this information in the methods section.

- *Please state when the HFS was given in respect to the conditioning (what means immediately before and after?) and in which context it was given. Were animals subjected to HFS exposed to the context longer (either before or after the conditioning while receiving HFS) than the other groups? When the HFS was given in another context (for the 24 h group)- how was this controlled for?*

Requested information has been added to the methods section. The control and intervention groups were treated in the same way.

- *When were the footshocks given in the anesthetized recordings (Fig. 4j) and how was the temporal relationship to the HFS? Was the timing the same as for the HFS in the behavioral experiments?*

Requested information has been added to the methods section.

- *Please add information on how the LFP was stimulated and how the LFP- EPSP slope was determined in in vivo recordings, likewise for the whole cell recordings of EPSPs in Fig. 5d-f.*

Requested information has been added to the methods section.

Here, the y-Axis in Fig. 5e should be corrected to EPSP slope rather than fEPSP slope if these are whole-cell recordings.

This has been corrected.

- *Please include information if the viral injections and opto-manipulations were done bilateral or unilateral and if so in which hemisphere. Likewise, indicate where the LFP recordings were done.*

Requested information has been added to the methods section.

- *Were there any exclusion criteria for animals (e.g. insufficient viral targeting or placement of fibers and electrodes), other than the testing of the optical CS for adverse effects?*

Requested information has been added to the methods section.

Statistics: In addition to clarifying analytical statistics, please clarify n-numbers for slice recordings (number of animals, number of slices, and number of cells if applicable).

Requested information has been added to the methods section.

It would be nice to scrutinize the results in extended data 4b. The freezing levels with U+24h HFS show a strong trend towards an increase, the effect size may be similar to immediate HFS Fig 4f and extended data 4a) if n was increased.

We agree with the reviewer. To address this point, we added “HomoLTP protocol when delivered 24hrs later, produced an increase in freezing; however, the value was not statistically significant.” To show this point, we used the same scale for freezing in Extended Data Fig. 4a and b.

In the final experiment (Fig. 5a-c), Fig. 5b seems to show results from only one animal, but behavioral results are from 4 animals (Fig 5c). It would be helpful to see the quantification of potentiation in each animal.

The results (now with error bar) include all mice.

Please spell out the abbreviation "STC".

Now, it is spelled out.

Page 8 last sentence of the discussion does not seem to fit there.

The sentence has been removed.

Reviewer #3 (Recommendations For The Authors):

(1) The authors did not determine how WTh affects Th-LA synapses, as field EPSPs were recorded only after HFS. WTh was required for the effects of HFS, as HFS alone did not produce CR in naïve and/or unpaired controls. As such the effects of the WTh protocol on synaptic strength must be investigated.

We have performed the experiment where we recorded the evoked LFP 2hrs and 24hrs following the weak conditioning protocol. We observed that a weak conditioning protocol that was not followed by an optical LTP protocol on the cortical inputs failed to produce synaptic potentiation of the thalamic inputs (tested 2hrs and 24hrs after the LTP protocol; Extended Data Fig. 5d,e).

(2) The authors provide some evidence that their dual opsin approach is feasible, particularly the use of sustained yellow light to block the effects of blue light on ChrimsonR. However, this validation was done using single pulses making it difficult to assess the effect of this protocol on Th input when HFS was used. Without strong evidence that the optogenetic methods used here are fault-proof, the main conclusions of this study are compromised. Why did the authors not use a protocol in which fibers

were placed directly in the Ctx and Th while using soma-restricted opsins to avoid cross-contamination?

We understand that the reviewer raises the possibility that our dual-opsin approach, although effective with single pulses, may fail in higher frequency stimulation protocols (10Hz and 85Hz). To address this concern, in a new group of mice we applied our approach to 10Hz and 85Hz stimulation protocols. We show that our approach is effective in single-pulse as well as in 10Hz and 85Hz stimulation protocols (Fig. 2d-h).